Journal of Marine Research, 58, 165–202, 2000

Journal of
MARINE RESEARCH

Volume 58, Number 2

The linkage between Upper Circumpolar Deep Water (UCDW) and phytoplankton assemblages on the west Antarctic Peninsula continental shelf

by Barbara B. Prézelin[1], Eileen E. Hofmann[2], Claudia Mengelt[1] and John M. Klinck[2]

ABSTRACT

Intrusion of Upper Circumpolar Deep Water (UCDW), which was derived from the Antarctic Circumpolar Current (ACC), onto the western Antarctic Peninsula (WAP) shelf region in January 1993 provided a reservoir of nutrient-rich, warmer water below 150 m that subsequently upwelled into the upper water column. Four sites, at which topographically-induced upwelling of UCDW occurred, were identified in a 50 km by 400 km band along the outer WAP continental shelf. One additional site at which wind-driven upwelling occurred was also identified. Diatom-dominated phytoplankton assemblages were always associated with a topographically-induced upwelling site. Such phytoplankton communities were not detected at any other shelf location, although diatoms were present everywhere in the 80,000 km^2 study area and UCDW covered about one-third the area below 150 m. Phytoplankton communities dominated by taxa other than diatoms were restricted to transition waters between the UCDW and shelf waters, the southerly flowing waters out of the Gerlache Strait, and/or the summertime glacial ice melt surface waters very near shore. We suggest that in the absence of episodic intrusion and upwelling of UCDW, the growth requirements for elevated silicate/nitrate ratios and/or other upwelled constituents (e.g. trace metals) are not sufficiently met for diatoms to achieve high abundance or community dominance. One consequence of this is that the ice-free regions of the outer WAP continental shelf will not experience predictable spring diatom blooms. Rather, this region will experience episodic diatom blooms that occur at variable intervals and during different seasonal conditions, if the physical structuring events are occurring.

Preferential drawdown of silicate relative to nitrate was observed at each of the offshore upwelling sites and resulted in a reduction in the ambient silicate:nitrate ratio relative to the corresponding value

1. Marine Science Institute and Department of Ecology, Evolution and Marine Biology, University of California, Santa Barbara, California, 93106, U.S.A. ***email: barbara@icess.ucsb.edu***

2. Center for Coastal Physical Oceanography, Old Dominion University, Norfolk, Virginia, 23529, U.S.A.

for unmodified UCDW (1.5 versus 3.0 for UCDW). The magnitude of the nutrient drawdown in areas of topographically-induced upwelling suggested that diatom growth had been elevated in response to recent upwelling but that the resulting increased algal biomass was either dispersed by advective processes and/or consumed by the larger krill that were observed to be associated with each offshore upwelling site. Thus, diatom bloom conditions on the outer WAP shelf may not be recognized based on elevated biomass and/or rates of carbon fixation. It was likely that similar physical forcing of significant phytoplankton growth, especially diatoms, may occur but be undetected in regions where the southern boundary of the ACC nears the Antarctic continental shelf edge. Our analyses from the west Antarctic Peninsula demonstrate coupling of the structure of the physical environment with nutrient distributions and phytoplankton assemblages and through to the higher trophic levels, such as Antarctic krill. This environment-trophic coupling may also occur in other regions of the Antarctic, as suggested by correspondences between the distribution of Southern ACC boundary and regions of high concentrations of Antarctic krill. The many mechanisms underlying this coupling remain to be determined, but it was clear that the ecology and biology of the components of the marine food web of the Antarctic continental shelf cannot be studied in isolation from one another or in isolation from the physical environment.

1. Introduction

The majority of the Southern Ocean is believed to have low plant biomass dominated by nanophytoplankton throughout the year (cf. von Bröckel, 1981; El-Sayed, 1987; Perrin *et al.,* 1987; El-Sayed and Fryxell, 1993; Smith *et al.,* 1996). Episodic blooms of both nano- and net-phytoplankton commonly occur in surface waters along the edge of the receding marginal ice (cf. Nelson and Smith, 1986; Wilson *et al.,* 1986; Smith 1990a,b; Prézelin *et al.,* 1994), and in polynas (cf. Smith and Gordon, 1997). These blooms also occur at oceanic fronts (de Baar *et al.,* 1995) and in nearshore straits, bays, and lees of islands (cf. Smith 1990b; Holm-Hansen and Mitchell, 1991; Holm-Hansen and Vernet, 1992; Priddle *et al.,* 1994; Bidigare *et al.,* 1996; Moline and Prézelin, 1996). These high biomass locations are considered critical feeding sites for higher trophic levels and major sites for biogeochemical cycling of nutrients. With the exception of cryptophyte blooms associated with glacial melt water (cf. Mura *et al.,* 1995; Moline and Prézelin, 1996), the community composition of these phytoplankton blooms tends to be dominated by diatom or by prymnesiophytes (e.g., *Phaeocystis* spp.). Chlorophytes and phytoflagellates (e.g. pelagophytes formally known as chrysophytes, dinoflagellates and prasinophytes) are also sometimes present (cf. Bidigare *et al.,* 1996; Moline and Prézelin, 1996, 2000).

Studies of these Antarctic open ocean, marginal ice edges and nearshore coastal sites have suggested that variability in phytoplankton biomass, community composition and/or primary production of these waters result from the combined effects of water column stratification, temperature, light regulation, and macro- and micronutrient limitation (cf. Smith and Sakshaug, 1990; Mitchell and Holm-Hansen, 1991; Sakshaug *et al.,* 1991; Tréguer and Jacques, 1992; El-Sayed and Fryxell, 1993; Prézelin *et al.,* 1994; de Baar *et al.,* 1995; Bidigare *et al.,* 1996; Moline and Prézelin, 1996, 1997, 2000). In this regard, these generalizations are consistent with those for other open ocean and high latitude systems (cf. Smith, 1990a,b; Valiela, 1995; Hutchins and Bruland, 1998). By comparison,

the coupling of physical, chemical and biological dynamics is essentially unknown for the less studied but extensive continental shelf waters that surround the Antarctic continent.

One of the better studied portions of the Antarctic continental shelf is the region to the west of the Antarctic Peninsula (cf. Ross *et al.,* 1996). Aspects of the biological, chemical and physical environment of this region have been studied intermittently for many years. The shelf is relatively deep (200 to 500 m) and has a rugged bottom topography (Fig. 1) and is about 200 km wide. Also, the continental shelf of the west Antarctic Peninsula (WAP) has a water mass structure that is essentially oceanic in character (Hofmann *et al.,* 1996; Smith *et al.,* 1999) and is influenced by variability of the Antarctic Circumpolar Current (ACC) which flows along the shelf break (Hofmann and Klinck, 1998a).

The opportunities for wind-driven nutrient upwelling are few as the overlying wind fields in austral summer favor downwelling circulation on the continental shelf in this region (Hofmann *et al.,* 1996). Therefore, it might not be surprising that the limited historical data indicate that these shelf waters, when not coincident with the retreating marginal ice zone in the spring, are generally characterized by low phytoplankton biomass. However, our observations of this area during 5 cruises from 1990 to 1993 indicate that the overlying shelf/slope regions in waters west of the Antarctic Peninsula are often characterized by a silicate drawdown of significant magnitude that seemed to coincide with a shift to increasingly diatom-dominated communities (Sullivan *et al.,* 1994; this study and Prézelin, unpubl. data). Thus, the nutrient depletion of these waters suggests there must be conditions on the shelf that favor diatom growth at levels exceeding those predicted from biomass and carbon fixation rates alone and sufficient to maintain the large and diverse populations of Antarctic krill, fish, marine mammals and benthic fauna in this region (Fraser and Trivelpiece, 1996; Costa and Crocker, 1996; Kellerman, 1996).

The goal of this study is to show cause and effect relationships between the hydrographic structure of shelf/slope waters and the phytoplankton community assemblages for a region of the WAP (Fig. 1). The hydrographic, chemical and phytoplankton data sets are the result of studies of the region done as part of a larger multidisciplinary study (Smith *et al.,* 1995). These data, in combination with knowledge of the bottom topography as well as slope/shelf water mass structure and wind direction and speed (Fig. 2), enable us to describe the environmental and biological structure of this region and to begin to determine the processes underlying this structure.

2. Methods

a. Sampling design and schedule

Station transects were aligned parallel to a southernmost across-shelf transect (the 000 Line) and perpendicular to a baseline which defines the inshore extent of the grid (Fig. 1). Each across-shelf transect was named in terms of its distance in kilometers from the 000 Line and each station along a particular transect was named in terms of its distance from the baseline. Working aboard the R/V *Polar Duke,* the January-February 1993 cruise occupied the region between the 600 and 200 Lines and included additional stations around

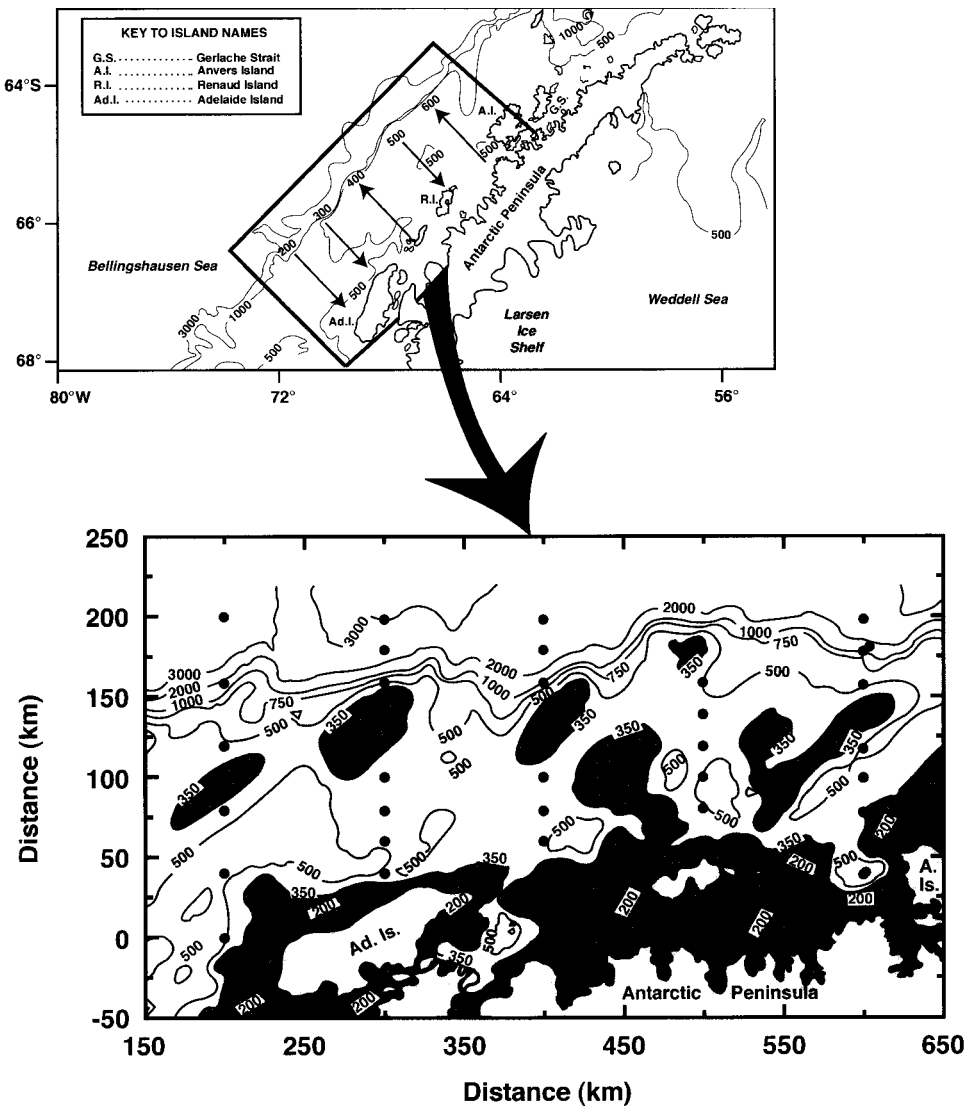

Figure 1. (Top) Map showing the locations of the sampling transects occupied during January 1993. Arrows indicate the direction of occupation of the transects. Bathymetric contours at 500, 1000 and 3000 meters are shown. (Bottom) Enlargement of the study area showing detailed bathymetric contours from 200 to 3000 m. Depths shallower between 350 and 200 m are indicated by the gray shading; depths shallower than 200 m are indicated by black. Locations of the stations along the across-shelf transects are indicated by the filled circles.

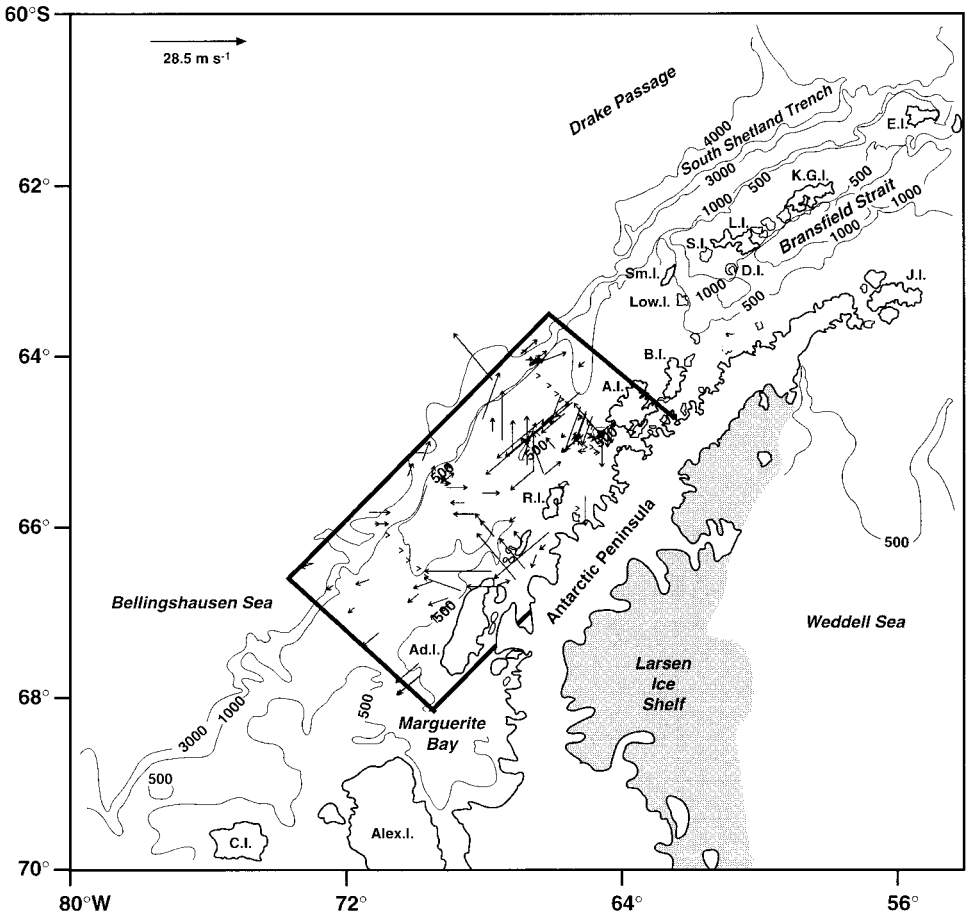

Figure 2. Wind vectors obtained from shipboard observations in January–February 1993. The vectors indicate the directions from which the wind was blowing.

Anvers Island that were not part of the basic transect design. These stations were occupied rapidly to give synoptic coverage of this region.

The austral summer time series and survey cruise was carried out in three phases. Surveys of the Palmer (600) and Renaud (500) transect lines were conducted from January 8 to 18, 1993 (Phase I), and, at each station, discrete samples were collected at several depths for determinations of major macronutrients, phytoplankton pigments, and hydrographic properties. Similar surveys of the Adelaide (400), Watkins (300) and Rothera (200) transect lines were conducted from January 25 to February 8, 1993 (Phase III). Sampling frequency was typically five to six stations per day (e.g., 4 to 5 hours between stations) which were located at intervals of 20 km. It is the survey data which are the basis of the present analyses.

Phase II activities (January 18 to 25, 1993) were transect surveys that focused on intensive vertical sampling of the Palmer Basin near Anvers Island and nearshore marine environments. Sampling included a ''fast track'' with 10 km spacing and a ''slow track'' with a 20 km spacing within a 50 km by 50 km grid west southwest of Palmer Station, located on Anvers Island. As sampling for nutrients and pigments was confined to the surface water (5 m), the Phase II data serve as a reference in the present study but are not part of the analyses presented here. Before, between and after each transect survey, a fine grid was also sampled around the islands in proximity to Palmer Station. Similarly, these fine grid data serve as a reference to the present study, but are not part of the analyses presented here.

b. Hydrographic samples

Along each transect, conductivity-temperature-depth (CTD) measurements were made at 20 km intervals using a SeaBird CTD mounted on a Bio-Optical Profiling System (BOPS) (Smith *et al.,* 1984). Vertical profiles were made to within a few meters of the bottom or to 500 m in deeper waters. Water samples were taken at discrete depths, analyzed for salinity with a Guildline Salinometer, and referenced to IAPSO standard seawater after return to Palmer Station. Pre- and post-cruise calibrations by SeaBird Electronics and comparison with the discrete salinity samples showed no significant drift in the temperature and conductivity sensors with time or depth. Thus, no corrections were made to the temperature and conductivity data. The hydrographic data were processed using the procedures and algorithms given in UNESCO (1983). Complete descriptions of the sensor calibrations and data processing were given in Lascara *et al.* (1993a).

The potential temperature and salinity data obtained from the CTD measurements were used to calculate the derived properties of potential density (σ_0) and the Brunt-Väisälä frequency (N^2). The latter quantity, which is a measure of water column stability, was used to determine the depth of the mixed layer at each station. Mixed-layer depth was defined to be the maximum in the Brunt-Väisälä vertical profile in the upper 150 m of the water column. At some stations, vertical profiles revealed multiple maxima in the Brunt-Väisälä frequency, indicating a complex mixing history. For these locations, the deepest Brunt-Väisälä frequency maximum was taken to be the depth of the mixed layer.

Whenever possible the spatial resolution of the temperature field was increased by using Expendable Bathythermograph (XBT) probes, which were deployed halfway between transect stations. Additional XBT measurements provided coverage of the region around Anvers Island during the Phase II survey. All XBT data were collected using T-6 (nominal maximum depth of 460 m) or T-7 (nominal maximum depth of 760 m) Sippican probes that were deployed with either a hand-held or deck-mounted launcher while underway. A complete description of the XBT data collection and post processing was given in Lascara *et al.* (1993b).

Throughout the cruise, wind direction and speed were recorded at hourly intervals by the meteorological sampling package located aboard the R/V *Polar Duke.* These data were

corrected for ship speed and direction and decomposed into north-south and east-west vector components. The resultant hourly values were daily averaged and recombined to obtain wind vectors along the ship track (Fig. 2). Thus, the wind vectors along the 500 Line and outer portion of the 400 Line were predominately upwelling favorable.

c. Nutrient determinations

Water samples were collected at discrete depths using 5-L Go-Flo bottles. Replicate subsamples for nutrient determination were filtered within an hour of collection through a 0.4 µm pore diameter polycarbonate filter. Samples were then frozen at −20°C and transported to the Marine Science Analytical Laboratories, University of California, Santa Barbara, for nutrient analyses according to the methods of Johnson *et al.* (1985).

d. Pigment determinations

Chlorophyll and carotenoid concentrations were determined for 660 samples collected during CTD vertical profiles at transect stations spaced 20-km apart along the 200 to 600 transect lines (Fig. 1A). Samples were collected in 5-L Go-Flo bottles and filtered on 0.4 µm nylon 47 mm Nuclepore filters and extracted in 3 ml of 90% acetone for 24 hr in the dark at −20°C. Pigment determinations were made at sea using reverse-phase HPLC procedures detailed in Wright *et al.* (1991), with the aid of an Hitachi(r) L-6200A pump and an L-4250 UV/VWAS variable wavelength detector (436 nm) equipped with a Waters Resolve C18 column (3.9 × 300 mm, 5 mm). Peak identities of algal extracts were determined by comparing their retention times with pure pigment standards.

The distribution pattern of pigment abundances along each transect line was generated using Fortner's Transform PPC (version 3.3.1), with contour scale matrices of 20 km × 25 m. The horizontal scale equals the distance between sampling profiles. The pigment contours were not extrapolated over the entire area of the 200 km × 200 m transect lines but rather were limited to more accurate estimates within boundaries of the data. This conservative approach better represented the spatial scales over which the physical, biological and chemical data were linked than did pigment distributions generated using larger matrices (unpubl. data).

e. Evaluation and selection of potential chemotaxonomic markers

An estimate of phytoplankton community composition first depends upon the choice of chemotaxonomic marker pigments (Table 1). Chlorophyll *b* and the carotenoids 19′-hexanoyloxy-fucoxanthin (HEX), 19′-butanoyloxy-fucoxanthin (BUT), fucoxanthin (FUCO) and peridinin (PERI) are commonly employed biomarkers indicating the specific presence of chlorophytes, prymnesiophytes, pelagophytes, diatoms and dinoflagellates, respectively. However some of the major carotenoids in one algal group may also occur as secondary pigments in members of other algal grouping(s) (Jeffrey *et al.,* 1997). Where this occurs, the potential for some confusion or uncertainty in the estimates of phytoplankton community composition exists. The exception is peridinin, which is the exclusive chemo-

Table 1. Summary of photosynthetic pigment distributions among marine phytoplankton. Pigments in bold are diagnostic markers (Bidigare *et al.,* 1996).

Algal group	Major pigments present
Prokaryotic phytoplankton	
Prochlorophytes	**Divinyl chlorophyll *a* and *b*,** monovinyl chlorophyll *b*, zeaxanthin, α-carotene, chlorophyll *c*-like pigment
Cyanobacteria	Monovinyl chlorophyll *a*, zeaxanthin, **phycoerythrin,** β-carotene
Eukaryotic phytoplankton	
Diatoms	Monovinyl chlorophyll *a*, chlorophylls *c*1 and *c*2, **fucoxanthin,** diadinoxanthin, diatoxanthin, β-carotene
Prymnesiophytes	Monovinyl chlorophyll *a*, chlorophylls *c*2 and *c*3, **19′-hexanoyloxyfucoxanthin,** fucoxanthin, diadinoxanthin, diatoxanthin, α- and β-carotene
Pelagophytes*	Monovinyl chlorophyll *a*, chlorophylls *c*2 and *c*3, **19′butanoyloxyfucoxanthin,** fucoxanthin, diadinoxanthin, diatoxanthin, β-carotene
Cryptophytes	Monovinyl chlorophyll *a*, chlorophyll *c*2, **alloxanthin,** phycoerythirin, α-carotene
Dinoflagellates	Monovinyl chlorophyll *a*, chlorophyll *c*2, **peridinin,** diadinoxanthin, β-carotene
Prasinophytes	Monovinyl chlorophyll *a* and *b*, **prasinoxanthin,** chlorophyll *c*-like pigment (Mg 3, 8 DVP a5), neoxanthin, violaxanthin, β-carotene
Chlorophytes	Monovinyl chlorophyll *a* and *b*, **lutein,** neoxanthin, violaxanthin, antheraxanthin, zeaxanthin, α- and β-carotene

*Formally called aberrant Chrysophytes.

taxonomic marker for dinoflagellates and does not occur in any other phytoplankton group. An evaluation of chemotaxonomic pigment markers, as detailed below, indicates that potential errors in estimates of phytoplankton community composition that arise from crossover pigmentation are small in this study and do not impact the general results and conclusions.

HEX is the biomarker for prymnesiophytes, a group of small flagellated phytoplankton that are widespread, very abundant, and an important part of the phytoplankton ecology in the Southern Ocean (cf. Bidigare *et al.,* 1996). This group includes coccolithophorids and other haptophytes. The best known Antarctic prymnesiophytes are *Phaeocystis* spp., often associated with seasonal blooms.

BUT is the biomarker for pelagophytes, which are small phytoflagellates previously known as crysophytes. However, BUT also occurs in some Antarctic *Phaeocystis* spp. (Wright and Jeffrey, 1987; Buma *et al.,* 1990; Nichols *et al.,* 1991; Vaulot *et al.,* 1994). In eight laboratory cultures of *Phaeocystis,* BUT concentrations were 1–13% of HEX concentrations. In one additional *Phaeocysti* culture, BUT concentrations were 30% of HEX concentrations. These studies also showed that the HEX:BUT ratio within some

Phaeocystis spp. is not fixed but can vary with change in growth conditions (Wright and Jeffrey, 1987; Buma *et al.*, 1990; Nichols *et al.*, 1991; Vaulot *et al.*, 1994).

Microscopic examinations of the phytoplankton collected during the January-February 1993 cruise indicated prymnesiophytes and pelagophytes often co-occurred over the continental shelf of the WAP (Prézelin *et al.*, 1994; Moline and Prézelin, 1996; unpubl. data). If a high percentage (e.g. 10%) of the BUT signal in the pigment samples is attributable to prymnesiophytes rather than pelagophytes, then the contribution of pelagophyte BUT to the total of carotenoid biomass (diatom FUCO, prymnesiophyte HEX, and pelagophyte BUT) decline 1.10 ± 0.6%. The remaining 99% BUT assignable to pelagophytes would be, on average, 12.1% (range 2.3% to 30.3%) instead of 13.3% (range 2.6% to 32.6%) of the total HEX + BUT + FUCO biomass in any discrete sample. Thus, the impact of sharing of BUT pigmentation between pelagophytes and prymnesiophytes is likely quite small in this study where FUCO and HEX were the two most abundant phytoplankton pigments after Chl *a*.

Fucoxanthin is the chemotaxonomic marker for diatoms. However, small amounts of FUCO may be present as secondary carotenoids in some but not all prymnesiophytes and pelagophytes. For some of the laboratory grown *Phaeocystis* spp. discussed above, FUCO concentrations averaged 15 ± 3% of HEX + BUT concentrations (Wright and Jeffrey, 1987; Buma *et al.*, 1990; Nichols *et al.*, 1991; Vaulot *et al.*, 1994). In field samples of mixed phytoplankton, the fraction of FUCO in different algal groups cannot be determined at present. However, we can make use of laboratory findings to estimate the upper limit for nondiatom FUCO. Assuming that nondiatom FUCO in a phytoplankton community equaled 10% of the HEX + BUT concentrations (a high value considering there are many prymnesiophytes and pelagophytes which contain no FUCO), then the remaining FUCO assignable to diatoms would decrease by an average of 2.3% ± 0.5% ($n = 660$) in the present study. If FUCO concentrations are reduced 2.3%, then regression analyses of community composition would reduce the estimate of diatoms by a few percent in regions where FUCO is the dominate pigmentation and by ca 5–7% in regions where HEX + BUT are the dominate pigmentation. This evaluation suggests that the impact of crossover FUCO pigmentation on estimates of the percent contribution of diatom to diatom-dominated communities would be minimal while estimates of the percent contribution of phytoflagellates in nondiatom-dominated communities would increase slightly.

The combined biomass of diatom FUCO, prymnesiophyte HEX, and pelagophyte BUT generally accounted, on average, for 98 ± 5% ($n = 660$ with a range = 68% to 100%) of all carotenoid marker pigmentation in any discrete sample. FUCO accounted for 52.9 ± 16.6%, HEX for 33.9 ± 14.5%, and BUT for 13.3 ± 5.9% of total carotenoid markers (Table 1). The large standard deviations reflect the uneven and dissimilar distribution of these pigments across the WAP continental shelf (Plate 1). HEX + BUT always co-occurred. The percentage of HEX/HEX + BUT in any one sample ranged widely, from 20% to 90% with an average of 79% ± 11% ($n = 660$).

Chlorophyll *b* is present in chlorophytes, prasinophytes and prochlorophytes (cf. Jeffrey

et al., 1997). Assigning this marker pigment to any one group can be challenging, requiring that the distribution of other marker pigments be considered simultaneously. The distribution of rarer pigments is useful in assigning Chl *b* because these pigments are often excellent indicators of boundaries of different hydrographic conditions. These hydrographic boundaries are important considerations when subsetting pigment data in order to obtain more robust estimates of phytoplankton community composition.

In the present analyses, we first eliminated prochlorophytes as a source of Chl *b* because this group has not been observed in the Southern Ocean in spite of efforts to do so using flow cytometry (R. Olson, pers. comm.). The assumption was supported by indirect pigment data. Chl *b* was present in 36% of the transect samples. About half of these samples contained more than one of the marker pigments (prasinoxanthin, zeaxanthin and lutein) which co-occur with Chl *b* in different phytoplankton groups. Prasinoxanthin, a specific biomarker for prasinophytes, only co-occurred with Chl *b* but was present in only 13% of the Chl *b* samples (or 5% of the total samples) and none of these contained zeaxanthin. Where prasinoxanthin was present, lutein was also present in about equal quantities.

Zeaxanthin also always co-occurred with Chl *b* and 89% of these samples also contained lutein but never prasinoxanthin. These observations suggest that chlorophytes (which contain Chl *b*, zeaxanthin and lutein) accounted for most of the Chl *b* biomass in these locations. The possible likelihood of zeaxanthin-containing cyanobacteria was low. There were no instances where zeaxanthin occurred in the absence of Chl *b*, as one might expect if planktonic cyanobacteria were present and differentially distributed from chlorophytes.

The remaining half of the Chl *b* samples did not contain any detectable levels of lutein, prasinoxanthin or zeaxanthin. Almost all of these samples were collected at depths $>$50 m, whereas shallower Chl *b* samples contained lutein. As a result, lutein: Chl *b* ratios tended to increase close to the surface. This observation is consistent with lutein's known role as a high light-induced photoprotective pigment in chlorophytes. We suggest that the deep water Chl *b*, in the absence of any lutein (or prasinoxanthin and zeaxanthin), can be attributed to the presence of low light adapted chlorophytes. If true, then lutein distribution, a traditional biomarker for chlorophytes, does not provide a complete picture of this group's distribution in WAP coastal waters.

Lastly, a comment regarding cryptophyte pigment distribution is warranted as cryptophytes are known to be very abundant in inshore surface melt waters during the spring and summer (Mura *et al.,* 1995; Moline and Prézelin, 1996) and are increasingly thought to be indicators of climate change in the Southern Ocean (Moline and Prézelin, 1996). The cryptophyte chemotaxonomic marker (alloxanthin) was detected at low concentrations in two spatially restricted locations during the austral summer cruise. Cryptophytes co-occurred with prasinophytes and chlorophytes in a patch of low salinity surface waters transected between the 500 and 600 Line. This data set is not included in the present analyses. A large but very dilute region of cryptophytes was also detected 30–80 m offshore along most of the 200 Line, along most of the 300 Line (stations 300.40–300.120)

and at the mid-portion of the 400 Line (stations 400.60–160). It is tempting to suggest that this large dilute region of cryptophytes may be the remnants of the bloom population that dominated local glacial melt waters just a few weeks prior (Moline and Prézelin, 1996).

f. Phytoplankton community composition

The above analyses allows the most abundant phytoplankton groups to be defined as: FUCO, the marker pigment for diatoms; HEX + BUT, the combined markers for prymnesiophytes + pelagophytes, that are hereon referred to as phytoflagellates; Chl *b*, the marker pigment for chlorophytes; and peridinin, the marker pigment for dinoflagellates. Multiple linear correlation analysis was used to derive coefficients for each pigment marker which was employed to calculate the fractional percent of total Chl *a* in each of these four taxonomic groupings (Table 2). A pigment coefficient (a_n) usually changes if there is a significant change in phytoplankton community composition and/or in the physiological, especially photoadaptive, state of the phytoplankton represented by the marker pigment. The predictive reliability of the estimates of pigment coefficients is partially assessed by comparing total measured Chl *a* with the sum of modeled Chl *a* contribution derived for each algal grouping within each discrete sample.

Early on, it became evident that two factors seriously degraded the predictive accuracy of the regressions: the inclusion of very dilute pigment concentrations and the blending of pigment data sets from locations with significantly different hydrographic conditions. The regression degradation due to very low pigment values arose because weighting toward the more abundant markers was not included in the analyses. The regressions were also strongly influenced by the numerous very small values for several pigments in many samples. Regressions significantly improved when pigment concentrations <10 ng L^{-1} were excluded. This concentration was a conservative estimate of the HPLC pigment detection limits. Regressions also improved significantly when rarer carotenoids were eliminated entirely from the regression analyses. For this study, carotenoids whose total concentration accounted for less than 1% of the total carotenoid biomass within any given data subset were eliminated from the final regressions for that data subset. During the austral summer cruise, prasinoxanthin and alloxanthin accounted for less than 1% of the total carotenoid biomass within our data subsets and were not considered in any regression analyses.

The following equation was used to perform multiple linear correlation analyses on the discrete pigment samples collected during the austral summer of 1993:

$$[\text{Chl } a]_{\text{tot}} = a_1[\text{FUCO}] + a_2[\text{HEX} + \text{BUT}] + a_3[\text{Chl } b] + a_4[\text{PERI}]. \quad (1)$$

The influence of hydrography on the regression analyses and prediction of phytoplankton community composition is summarized in Table 2. Distinct regressions were required for different regions of the shelf as well as for different physical layers within the water column. Regression analyses of Phase I (600–500 Lines) and Phase III (400–200 Lines) were carried out separately, in part because there was a break between Phase I and Phase III

Table 2. Results of multiple regression analyses performed on discrete measurements of taxonomic pigment concentrations sampled between the surface and 200 m over the continental shelf of the west Antarctic Peninsula during austral summer of 1993. Also presented are the coefficients derived from the regression formula Chl *a*tot = a_1(FUCO) + a_2 (HEX + BUT) + a_3(Chl *b*) + a_4(PERI) (Eq. 1) for pigments representing diatoms and phytoflagellates in the present study as described in the Methods. Comparisons are made of results of analyses performed on different subsets of the data sorted on the basis of cruise phase and hydrographic groupings. Further subdivision of Phase I regressions were based upon initial estimates of phytoplankton groupings. Shaded areas represent algorithms employed for calculations of phytoplankton community.

		Measured vs Modeled							
			Chlorophyll *a*			Derived Coefficients			
	Line code	*n*	Slope	Intercept	r^2	FUCO	HEX + BUT	PERI	CHL *b*
A	**Entire Data Set**	622	0.53	136	0.40	0.68	2.03	—	0.83
B	Only within FWL	22	1.13	−107	0.58	0.71	3.97	13.9	0.06
C	Excluding FWL	600	0.81	90	0.54	0.70	1.91	—	1.14
	Phase I (500–600)								
D	Including FWL	349	0.78	106	0.40	0.56	2.40	—	0.46
E	Excluding FWL	341	0.78	101	0.47	0.61	2.20	—	0.76
	Above MLD#								
F	Including FWL	190	0.89	66	0.59	0.89	1.56	7.85	0.44
G	Excluding FWL	182	0.89	59	0.62	0.85	1.55	5.58	0.77
H	• Pytoflag. >70%	12	0.90	26	0.79*	0.15	1.13**	<0.10	<0.10
I	• Remainder	170	0.89	61	0.71*	0.60	1.97	5.75	0.48*
J	• Diatoms >60%	45	0.96	9	0.84**	1.22**	0.26	—	<0.10
K	• Remainder	137	0.87	79	0.60	1.19	1.40	5.22	1.00
L	• 70% < Pytoflag. & <60% Diatoms	128	0.87	82	0.68	0.93	1.79	—	0.50
M	**Below MLD#**	45	0.06	375	0.00	1.32	0.91	—	<0.10
N	• Prym >70%	5	1.00	0	1.00***	<0.10	2.28***	<0.10	<0.10
O	• Remainder	40	0.74	76	0.49	1.12	1.40*	excl.	<0.10
P	• Diatoms >60%	20	0.99	3	0.87**	1.48**	<0.10	<0.10	<0.10
Q	• Remainder	25	0.78	73	0.76*	2.01*	0.70	0.40	<0.10
R	• <70% Prym & <60% Diatoms	23	0.75	84	0.74*	1.90*	0.86	<0.10	<0.10
	Phase III (200–400)								
S	Including FWL	273	0.92	46.70	0.83**	1.09	1.15	2.25	2.98
T	Excluding FWL	258	0.94	28.39	0.88**	1.07	1.22*	excl.	2.22
	Above MLD								
U	Including FWL	224	0.88	57.36	0.80**	1.10	1.11	2.27	3.65
V	Excluding FWL	209	0.93	36.55	0.87**	1.06	1.19	1.00	2.69
W	**Below MLD**	49	0.98	4.30	0.88**	1.18*	1.30	excl.	0.43*

Phytoflag. = prymnesiophytes + pelagophytes; FWL = Fresher Water Lens; MLD = Mixed Layer Depth.
# for stations where 24 hr profiling was carried out, only a single profile nearest mid-day was used in the regression calculations.
* for r^2 for regression of measured to modeled pigment is between 0.7-0.8.
** for r^2 for regression of measured to modeled pigment is between 0.8–0.9.
*** r^2 for regression of measured to modeled pigment is between 0.9–1.0.
excl. = excluded as PERI was <1.0% of total chemotaxonomic carotenoids in data sample.

to allow for fine-scale surface sampling in the very nearshore regions (Phase II) and, in part, because the quality of the regression analyses for Phase III improved significantly by doing so (Table 2 A, D, S). Further improvement was also noted when sparse data from the fresher water lens (FWL) was considered separately in regression of total (Table 2 A, C), Phase I (Table 2 D, E) and Phase III (Table 2 S, T) data sets. Within each Phase I and III data sets (excluding FWL data), separate regression analyses were made of data above and below the mixed layer depth (MLD). For Phase I, this subsetting of data improved regressions above the MLD (Table 2 E, G) while completely degrading regressions below the MLD. However, localized regions of very high prymnesiophyte (nearshore) or diatom (offshore) dominance occurred, respectively, above and below the MLD. When these localized communities were considered separately, regressions were significantly improved for the Phase I datasets representing regions above and below the MLD. For prymnesiophytes, compare Table 2 G, H, and I. For diatoms, compare Table 2 G, J and K. Subdivision by group dominance was not required for Phase III (excluding FWL) since regressions for data above or below the MLD were essentially the same as that for the combined datasets (Table 2 T, V, W). The final composite of phytoplankton community composition over the continental shelf of the WAP was based upon results from separate regressions for the FWL (Table 2 B), iterations of Phase I data above and below the MLD which kept coarser iterations of community composition in mind (Table 2 H, J, L), and Phase III data above and below the MLD (Table 2 V, W).

3. Results

a. Temperature maximum and nutrient ratio relationship

The distribution of the temperature maximum below 250 m for the WAP continental shelf waters during January–February 1993 (Fig. 3) showed a feature of the circulation of this shelf that was not appreciated until recently. The 1.8°C isotherm represented the southern boundary of the Antarctic Circumpolar Current (ACC) (Table 3) and was indicative of the UCDW being transported by the ACC at depths of 200–800 m (Hofmann and Klinck, 1998a; Smith *et al.,* 1999). Temperatures between 1.8°C and 1.5°C over the shelf were representative of a modified form of UCDW, which was formed from the mixing of UCDW with the cooler and fresher Antarctic Surface Water (AASW) (Smith *et al.,* 1999). Modified UCDW was found on much of the Antarctic continental shelf (Hofmann and Klinck, 1998b). The extent and magnitude of the UCDW on the WAP continental shelf was related to variability in the location of the southern boundary of the ACC along the shelf break (Hofmann and Klinck, 1998a). During January–February 1993, modified UCDW extended onshore in a band that essentially covered the outer to middle shelf of the study region (Fig. 3A).

The UCDW, which was derived from North Atlantic Deep Water, was high in nutrients. NO_3 values were 32–34 mmol m^{-3} and the $Si(OH)_4$ values were 100–105 mmol m^{-3}. The $Si(OH)_4$:NO_3 ratio provided a means of tracking the UCDW as it moved onto the WAP continental shelf. The $Si(OH)_4$:NO_3 molar ratio at 250 m, which corresponds to the

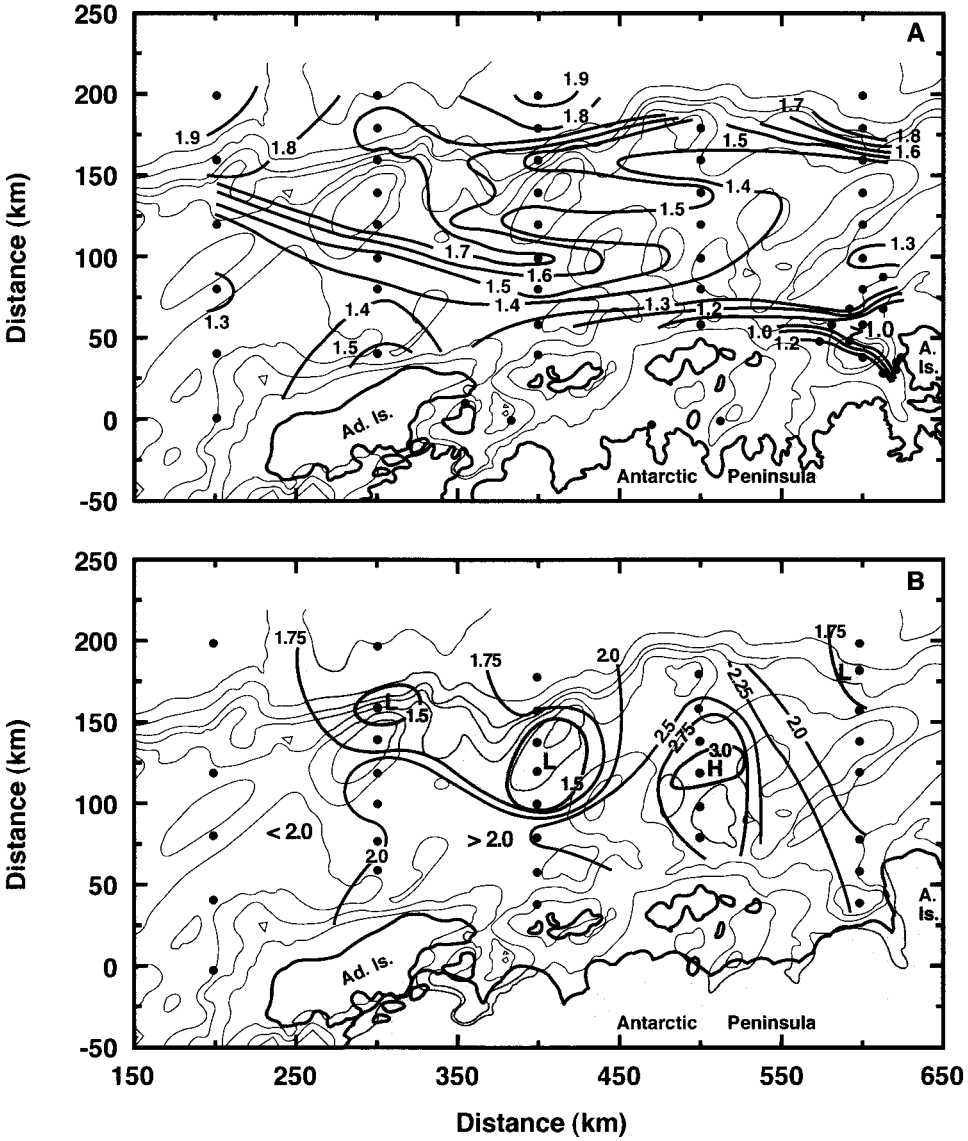

Figure 3.(A) Distribution of the temperature maximum below 250 m as constructed from temperature measurements made in January 1993. Figure adapted from Hofmann and Klinck (1998a). (B) Horizontal distribution of the ambient $Si(OH)_4$:NO_3 ratio at a depth of 200 m. Shading indicates areas where the ratio is less than 1.75 and areas where the ratio is greater than 2.75. Filled circles indicate station distribution and thin solid lines are bottom bathymetry in meters, identical to those displayed in Figure 1.

Table 3. List of abbreviations for Antarctic currents, fronts and water masses.

AASW	Antarctic Surface Water
ACC	Antarctic Circumpolar Current
Bndy	Antarctic Circumpolar Current Boundary
PF	Polar Front
SACCF	Southern Antarctic Circumpolar Current Front
SAF	Subantarctic Front
STF	Subtropical Front
UCDP	Upper Circumpolar Deep Water
WW	Winter Water

temperature maximum of the UCDW, would be expected to have values of 2.5 to 3.0. However, in January 1993, the $Si(OH)_4$:NO_3 ratios measured at 200 m within the 1.8°C and 1.5°C waters of the UCDW had values less than 2.0 (Fig. 3). At the outer shelf along the 300, 400 and 600 Lines, where the onshelf intrusion of UCDW originated, ambient $Si(OH)_4$:NO_3 ratios were 1.75 to 1.5 at 250 m (Plate 2 A, G, J). These lower than expected $Si(OH)_4$:NO_3 values were the result of significant silicate removal relative to nitrate removal (Figs. 6 and 7). The overlying water column at these locations had similarly low $Si(OH)_4$:NO_3 ratios that extended to the surface (Plate 2 A, G, J). Downward mixing of the nitrate and silicate concentrations associated with AASW was a possible explanation for the decreased nutrient ratios, but heat and salt budgets for the WAP shelf suggested that diffusive mixing was from the UCDW to the AASW (Smith *et al.*, 1999). Also, as shown later, the NO_3 and $Si(OH)_4$ concentrations of AASW were not sufficiently low to produce the observed 50% decrease in the $Si(OH)_4$:NO_3 ratio at 250 m. Thus it was reasonable to suggest that, at the time of our sampling, upwelling of the intruded UCDW had already introduced inorganic nutrients into the upper water column which was being or had been biologically utilized.

In contrast, the middle portion of the 500 Line showed $Si(OH)_4$:NO_3 ratios that were within the values expected for newly intruded UCDW that had not been biologically utilized (Plate 2D). These higher $Si(OH)_4$:NO_3 ratios were observed to extend to the surface at these locations, suggesting recently upwelled UCDW waters at this location. The time during which the high $Si(OH)_4$:NO_3 ratios were observed on the middle 500 Line coincided with a period of wind from the south-southeast (Fig. 2), which on the WAP shelf was upwelling favorable. Wind from this direction was not typical for the WAP shelf (Hofmann *et al.*, 1996) but this event followed, by about two days, the passage of a strong low pressure system, indicated by the large wind vectors observed near the 600 Line (Fig. 2).

The variation in the magnitude of the $Si(OH)_4$:NO_3 ratio suggested connections between hydrographic and biological processes related to phytoplankton growth in surface waters. To pursue this suggestion, the vertical distributions of temperature, salinity and pressure along the sampling transects were analyzed along with the corresponding vertical distributions of macronutrients, phytoplankton pigments and phytoplankton community composition. These analyses are described in the sections that follow.

b. Temperature, salinity and density vertical distributions

600 and 500 Lines. The vertical temperature distribution measured along the 600 Line (Fig. 4A) during Phase I showed UCDW at the outer shelf below 200 m. The cold water (<0°C) centered around 100 m was Winter Water (WW), which was the end member of the Antarctic Surface Water (AASW) that was formed by winter cooling. The WW extended as an almost continuous band across the shelf. The disappearance of this feature at the inner portion of the transect was due to upward mixing of UCDW from shallow bathymetry (Hofmann and Klinck, 1998b). Above the WW layer was the AASW, which undergoes modification due to local surface processes of heating and cooling and thus varies in structure across the shelf.

Below 300 m, salinity values greater than 34.65 ppt indicated the presence of UCDW at the outer shelf (Fig. 4B). Salinities between 34.5 and 34.6 ppt extended across the shelf, indicating the onshore extent of the modified UCDW. Above 60 m, there were two regions of low salinity water (<33.8 ppt) on the inner portion of the transect that may have originated from melting of glacial ice and/or sea ice from the previous winter. The low salinity water locations also corresponded to a region of the shelf that was influenced by outflow from the nearshore region around Anvers Island and outflow from the Gerlache Strait (Smith *et al.*, 1999).

The density surfaces below 200 m at the outer end of the 600 Line (Fig. 4C) tilted upward from off (600.200) to on-shelf (600.160). This pattern was consistent with the intrusion of UCDW onto the shelf at depth due to the onshelf movement of the southern boundary of the ACC (Hofmann and Klinck, 1998b). Over the shelf, the density surfaces were relatively flat below 100 m, except near shallow topography. The region of reduced density at the surface on the inner part of the 600 Line coincided with a FWL.

Along the 500 Line, temperature values below 200 m (Fig. 4D) did not exceed 1.25°C except for one small region at the outer shelf. This temperature distribution indicated that modified UCDW was present and that UCDW had not newly intruded onto the shelf at this location. The salinity and density vertical sections (Fig. 4E, F), however, suggested that at the middle and inner portions of this section, there was vertical displacement of the deeper waters upward. The low salinity water evident on the inner 600 Line was also present on the inner portion of the 500 Line, but was reduced in extent, as indicated by the distribution of the 33.8 ppt isohaline.

400, 300 and 200 Lines. The temperature structure on the 400, 300, and 200 Lines (Fig. 5A, D, G) showed water warmer than 1.5°C intruding onto the shelf below 150 to 200 m at the outer end of each section. Between 100 and 200 m the WW layer was a continuous feature across the shelf. Above the WW layer, the AASW showed little variation in temperature across the shelf. However, the salinity and density sections (Fig. 5) showed a region of fresher and less dense water at the innermost stations along all three transects.

The most extensive intrusion of UCDW occurred on the 300 Line, where water warmer

than 1.5°C was found at all but the innermost three stations (Fig. 5D). The extent of this intrusion of UCDW was represented by the distribution of the 34.7 ppt isohaline (Fig. 5E) and the 27.7 isopycnal (Fig. 5F). In addition, the 300 Line was the only location where water densities of 27.8 ppt, which corresponded to core UCDW, were found. Thus, the 300 Line captured a site of active UCDW intrusion during the January 1993 field sampling effort. In addition, UCDW was significant along the 200 Line at this time. These vertical sections suggested that UCDW intrusions had a spatial extent of at least 200 to 300 km and that the southern portion of the WAP study region may have been a preferred site for movement of UCDW onto the WAP.

c. Nutrient vertical distributions

600 and 500 Line. There was considerable across-shelf variability in vertical distributions of NO_3, $Si(OH)_4$ and PO_4 along the 600 and 500 Lines (Fig. 6). These macronutrients were generally much more abundant along the 500 Line than along the 600 Line. Lowest ambient concentrations of macronutrients were in the upper 100 m of the outer shelf region of the 600 Line, where the onshelf intrusion of the UCDW originated. The highest concentrations of macronutrients along the 600 Line were located, with the exception of station 600.040, below these overlying waters and where bathymetric upwelling of the UCDW had occurred. By comparison, $Si(OH)_4$ concentrations throughout water column at the mid-shelf region of the 500 Line were at about twice the high as those at corresponding locations on the 600 Line (Fig. 6B, E). Concentrations of NO_3 and PO_4 were about 30–40% higher on the 500 Line than at corresponding locations on the 600 Line. Thus, the nutrient structure in the upper 100 m along the 600 Line appeared to be largely determined by biological processes of nutrient uptake and, as shown below, especially by diatoms in the outer shelf region. In contrast, the nutrient structure above 100 m along the 500 Line at the time of sampling appeared to be largely determined by recent wind-driven upwelling events and only secondarily by biological processes.

400, 300 and 200 Lines. The across-shelf distribution of nitrate, silicate and phosphate in the upper 100 m along the 400, 300 and 200 Lines (Fig. 7) showed considerable variability with no distinct pattern. This was indicative of biological modifications and was consistent with the distribution patterns of Chl *a* biomass and chemotaxonomic marker pigments (Plate 1K–T). Below 150 m, the patterns in nutrient distributions were similar to those seen on the outer 600 Line. Increased concentrations of NO_3, $Si(OH)_4$ and PO_4 occurred at sites that corresponded to regions where UCDW was intruding onto the shelf. The vertical structure of the deeper nutrient fields again indicated upward transport from the UCDW.

Further quantitative analyses will be required to substantiate the patterns we have described, to quantify nutrient consumption ratios, and to assess when and where macronutrients and/or micronutrients are limiting phytoplankton growth and community composition. Results will also be important to assessments of patterns of primary production for the same data set. We have looked at the issues and recognize them to be

important but complicated to resolve. Thoughtful analyses of the nutrient data in the recently upwelled waters on 500 Line and the nutrient availability in the winter water (March and August, 1998) will be necessary to set the *n*-member from which the nutrient consumption ratios can be derived. One analytical complication will be incorporating the nutrient dilution effects brought on by glacial ice melting in the very nearshore waters as well as the precipitation associated with a major storm event during the study. Another complication will be the likely taxonomic differences in consumption ratios and carbon production. We are also aware of time series studies (Moline and Prézelin, 1994; 1996) that indicate phytoplankton in very nearshore waters sometimes display $Si(OH)_4$:NO_3 and $Si(OH)_4$:PO_4 draw down ratios that deviate significantly from Redfield ratios (16:1:15 nitrate:phosphate:silicate) and are comparable to ratios (11:1:24) reported by Jennings *et al.* (1984) in his study of phytoplankton in the Southern Ocean. There are also observations of NO_3:PO_4 ratios in diatom blooms may exceed 80 and suggests the possibility of phosphate limitation during periods of rapid growth (Moline and Prézelin, 1994; 1996).

d. Mixed layer depths and phytoplankton biomass

The vertical structure of the upper water column varied widely over the WAP shelf (cf. Figs. 4, 5). Of the sampling locations, 24% were designated as being without an obvious mixed layer in the upper 120 m, as determined by profiles of Brunt-Väisälä frequencies (N^2) with maximum values less than 0.5×10^{-5}. These stations were located very nearshore on the 600, 400 and 300 Lines (Plate 1). Along the upwelling region of the 500 Line, the maximum Brunt-Väisälä frequencies (N^2) of the station locations ranged from 0.5 to 0.9×10^{-5}. Highest water column N^2 values, ranging between 0.9 to 1.4×10^{-5}, were associated with MLDs on the outer continental shelf of the 600, 400, 300 and 200 Lines where the isopycnals sloped toward the surface. Where MLDs occurred, they were at ca 76 ± 12 m.

The spatial distribution of summertime Chl *a* biomass and MLDs along the 600 to 300 Lines (Plate 1 A, F, K, P) showed that over the continental shelf of the west Antarctic Peninsula, summertime Chl *a* biomass varied ca 20-fold with highest concentrations approaching 1200 ng L^{-1}. Variability in the biomass distribution occurred on horizontal space scales of less than 20–40 km along each transect line (including the 200 Line; data not shown). Assessment of the total data set indicated *no* correlation ($r^2 < 0.02$, $n = 29$) between a shallowing of the regional MLDs and increases in overlying integrated water column Chl *a*, FUCO or HEX + BUT. There was also *no* correlation ($r^2 < 0.02$) between MLDs and the percentage of the total phytoplankton assemblages represented by diatoms or phytoflagellates (data not shown). MLD was *not* the determinant of biological activity in this shelf region at this time of year; in fact quite the opposite. There was a *positive* correlation between MLDs and integrated Chl *a* biomass ($r^2 = 0.69$), as well as between MLDs and integrated FUCO ($r^2 = 0.87$) biomass.

e. Vertical pigment and phytoplankton distribution

600 Line. The effect of the hydrographic structure on phytoplankton communities was complex along the 600 Line. The transect showed influences of low salinity waters derived from the surrounding glaciers and contributing to the dynamics of a FWL, inflow from the Gerlache Strait at the inshore, a mixing event of the UCDW near shallow inshore bathymetry, previous upwelling of the UCDW on the outer shelf and advective intrusions in the mid-shelf region. Regression analyses for the phytoplankton community composition on the 600 Line accounted for the hydrographic complexity. Separate consideration was given to pigment distributions within FWL, above and below the MLD, and in subsets representing the small pockets in the regions where one group of phytoplankton accounted for the vast majority of the Chl *a* biomass (Table 2). The pattern of phytoplankton community composition was reconstructed by combining the outcomes of these analyses. The composited view of structure and relationship between the different phytoplankton groups along the 600 Line was far more robust than analyses based upon little or no consideration of the hydrographic influences partitioning phytoplankton assemblages into distinct regions of the shelf (Table 2).

There were three Chl *a* maxima in the surface waters along the 600 Line (Plate 1A). One of the Chl *a* max was detected in the upper 40 m near 600.040 (Plate 1A), which was located at the outflow of the Gerlache Strait and directly over a deep hole in the continental shelf (Fig. 1). This Chl *a* max (up to 850 ng L^{-1}) was also shoreward of a topographical rise at 600.060, where upward mixing of the UCDW and WW was occurring (Fig. 4A). A second Chl *a* max ($>$2100 ng L^{-1}) at ca 600.100 also extended from the surface, through a FWL and to a depth of about 40 m. Differences in the relative amounts of peridinin (Plate 1D) and Chl *b* (Plate 1E) within these two Chl *a* patches suggested differences in hydrographic conditions leading to the development of these small Chl *a* blooms. The third Chl *a* patch (up to 1600 ng L^{-1}) was in the upper 30 m at 600.140 and just above an intrusion of high $Si(OH)_4$:NO_3 waters (Plate 2A).

Elevated HEX + BUT and FUCO were present in equal abundances within the Chl *a* max at 600.140 (Plate 1B, C). At this location, the bathymetry was characterized by a topographical rise to a plateau within 350 m of the surface (Fig. 1B). Higher concentrations of FUCO and HEX + BUT were associated with deep maxima located in distinctly different water columns found on opposite sides of the submarine plateau. Moving shoreward, FUCO was dilute while more abundant HEX + BUT occurred in a deep maxima beneath surface Chl *a* maxima. The HEX + BUT maxima were located below the seasonal pycnocline, generally in association with MLD $>$ 120 m, and in nearshore areas where the UCDW was not detectable at 300 m. Seaward of the topographic rise at 600.140, HEX + BUT concentrations declined abruptly at the continental shelf break. However, FUCO concentrations increased below and seaward of the Chl *a* and the HEX + BUT maxima at 600.140. The FUCO maximum was associated with MLDs $<$ 70 m and in areas with upwelling of the UCDW (Fig. 4A).

The FWL was well developed in the nearshore region of the 600 Line at the time of sampling, a condition that may have been supported by a recent period of clear sunny days with low winds (Fig. 2). These waters were turbid due to the presence of glacial flour and contained 20–30% of water column Chl *a* biomass (Fig. 8). The remaining Chl *a* biomass was located in well-mixed waters below the FWL where the euphotic zone penetrated to less than half the upper mixed layer (Plate 3). The upper water column in nearshore region was characterized by high ambient $Si(OH)_4$:NO_3 ratios ($>$2.25, Plate 2A), and the drawdown of nitrate (Fig. 6A) appeared to be greater than that for silicate (Fig. 6B). These observations were consistent with a phytoplankton community composition with only 10–30% diatoms within the upper 80 m of the first 100 km of the 600 Line (Plate 2B). Conversely, phytoflagellates accounted for 72 $\pm$ 1%, ($n = 23$) of the phytoplankton biomass at any given depth throughout the upper 80 m, not including the FWL. Below 80 m, phytoflagellates became a smaller percentage of the community while diatoms became more predominant.

At the outer 600 Line, FWL communities were no longer evident and the phytoplankton assemblage throughout the water column began to shift away from dominance by phytoflagellates and toward diatom dominance. Most notable was the increased predominance of diatoms as the MLD shallowed and light penetration increased, eventually resulting in the entire upper mixed layer being within the euphotic zone (600.180–200). At the nearshore stations, diatoms were 28 $\pm$ 1% of the phytoplankton communities above the MLD, compared to 43 $\pm$ 10% at offshore stations. Dinoflagellates and chlorophytes occurred in the near-surface waters at the inner stations and reached 52 $\pm$ 7% of the total phytoplankton community at 600.200. Below the MLD at the offshore waters, diatoms routinely accounted for half the Chl biomass. It should be noted that increased percent dominance by diatoms did not translate into increased Chl *a* biomass accumulation at these sites (Fig. 8A).

The near-surface waters of the three stations where Chl *a* maxima occurred contained high light-adapted phytoplankton communities, characterized by a high proportion of photoprotective pigmentation and light requirements for maximal rates of photosynthesis that exceeded 150 to 200 uEin m^{-2} s^{-1} (Prézelin, unpubl.). The two inshore Chl *a* maxima were composed of high light phytoplankton communities within and just below the FWL. The offshore Chl *a* max also composed of high light-adapted phytoplankton communities within lower salinity surface waters. The community assemblages within the high light environments were similar in composition although the relative abundances of prymnesiophyte, dinoflagellates, chlorophytes and diatoms changed to a small degree from location to location (Plate 3, top row). These communities always contained abundant dinoflagellates and, on occasion, abundant chlorophytes. The upper 10 m of the water column was comprised, on average, of 41 $\pm$ 10% dinoflagellates, 41 $\pm$ 6% phytoflagellates, 12 $\pm$ 7% diatoms, and 6 $\pm$ 10% chlorophytes (Plate 3, top row).

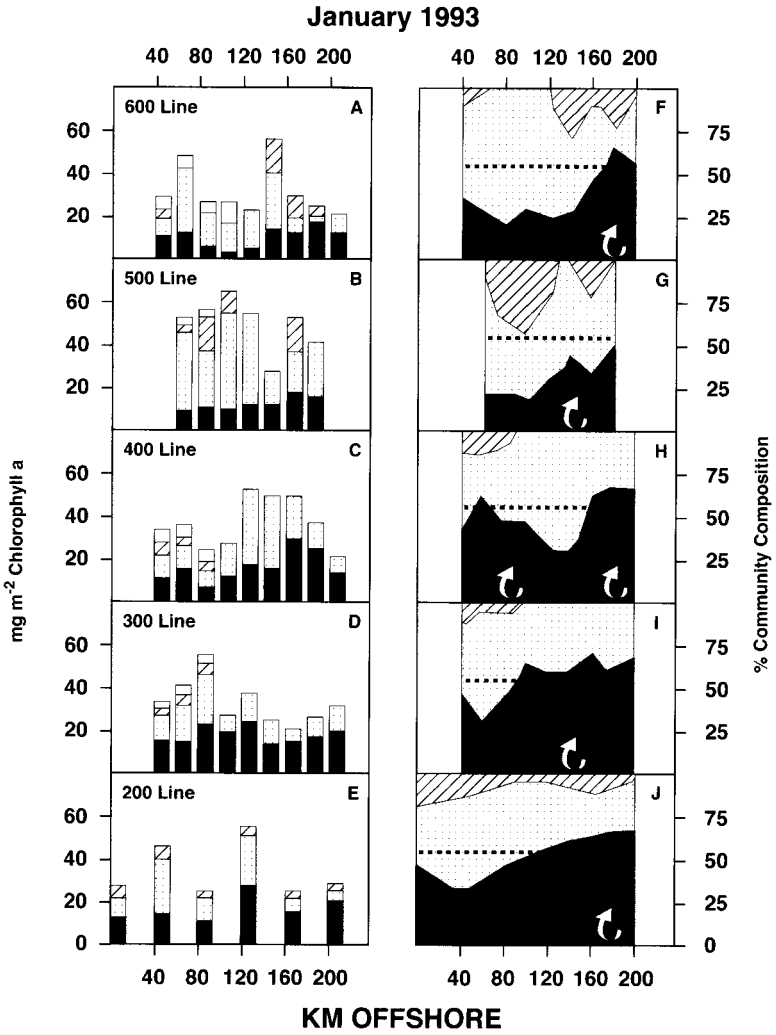

Figure 8. (Left) Comparison of integrated Chl *a* at discrete stations along 600–200 transect lines and its partitioning among biomass in the fresher water lens (blank bars), dinoflagellates + chlorophytes (bars filled with horizontal lines), prymnesiophytes + pelagophytes (speckled bars) and diatom (black bar). (Right) Percent distribution of total chlorophyll among different algal groups below the fresher water lens along the 600-200 transects area. Arrows indicate locations of upwelling.

500 Line. Wind-driven upwelling dominated the characterization of the hydrography and phytoplankton community structure along the 500 Line. Atypical winds from the south-southeast (Fig. 2) were associated with the passage of a low pressure system which produced strong (25–30 m s^{-1}) winds near the 500 and 600 Line about two days before the

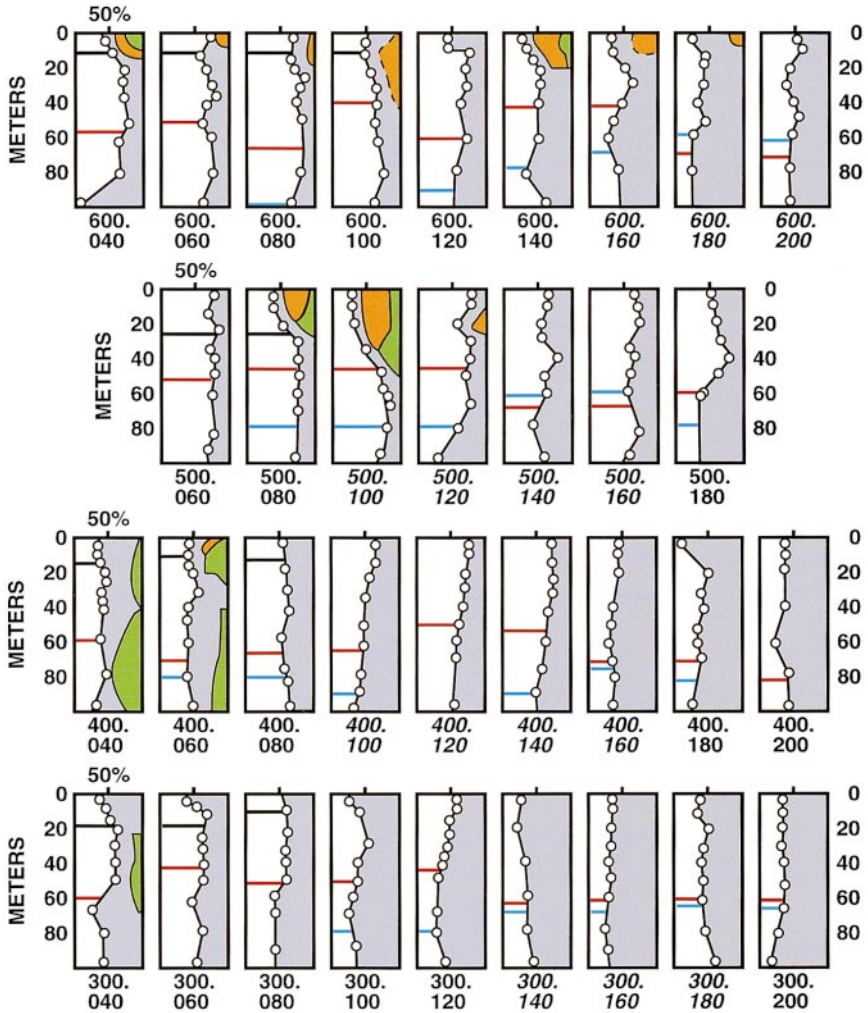

Plate 3. Comparison of vertical sections showing the distribution of the % contribution made by phytoflagellates (clear areas), diatoms (gray areas), dinoflagellates (orange areas) and chlorophytes (green areas) to overall phytoplankton community biomass from the 600 (top) to 300 (bottom) transect lines. On each vertical profile, the solid red line indicates the 1% light depth and the blue line indicates depth of the mixed layer. If a fresher water lens was present at the surface, the solid black bar indicates the approximate depth of this layer.

500 Line transect. The biological and chemical data suggest that the resultant wind-driven upwelling promoted diatom growth and dominance offshore while blurring the distinction between pre-existing inshore Chl *a* areas dominated by prymnesiophytes, pelagophytes and dinoflagellates. Furthermore, the two days between the low pressure system passage and occupation of the 500 Line appeared to be insufficient time for biological modification

of the nutrient ratios of the upwelled water to occur at the inshore locations. The lack of significant nutrient consumption in such high Chl *a* environments was possibly due to poor conditions for phytoplankton growth at the time of sampling. If so, the question remains whether the inshore nutrient-rich environment would eventually favor a shift toward diatoms as the physical and optical conditions for growth improved. The 500 Line transect provides insights into the complex and likely dynamics of phytoplankton community structure immediately following a major upwelling event on the WAP continental shelf as discussed below.

Relatively high Chl *a* concentrations were detected in the upper 40 m between 500.060 and 500.140 (Plate 1F, Fig. 8B). There was very little FUCO within the high Chl *a* distribution (Plate 1G); however, concentrations of HEX + BUT were elevated, especially subsurface and near the offshore boundary (Plate 1H). By comparison, Chl *b* was concentrated below 20 m (Plate 1J) and peridinin was concentrated in the upper 10–20 m in the area of the high Chl *a* distribution (Plate 1I). The differential distribution of phytoplankton pigmentation within the uniform distribution of high Chl *a* was an unusual observation and may reflect blurring of boundaries between previously discrete Chl *a* regions like those observed on the 600 Line prior to the storm. Some additional support for this suggestion comes from observations that the FWL on the 500 Line extended deeper (20 m) than, but not as far offshore as, the FWL on the 600 Line. Phytoplankton assemblages resembling those found within the FWL on the 600 Line were located at the outer edge of the FWL on the 500 Line as well as mixed deeper into the adjacent water column (500.100) that had no detectable FWL (Plate 3). The implication was that the FWL on the 500 Line was being degraded by recent mixing events.

Further support for recent mixing comes from ancillary assessments of the photophysiology of the phytoplankton communities. On the 500 Line, the turbidity of the FWL and higher Chl *a* biomass in inshore waters resulted in shallower euphotic zones (ca. 40 m) (Plate 3). Within these strongly attenuating light environments, the phytoplankton light-requirement (I_k) for maximal rates of photosynthesis stayed relatively constant from the bright light surface to ca. 30 m below the surface. The uniformity of I_k profiles at locations where photosynthetic light was strongly attenuated was highly indicative of recent or ongoing mixing of the water column (Prézelin *et al.,* 1991). This measure of the photoadaptive state of the phytoplankton responds to environmental light changes on time scales of a few hours to a few days depending upon growth conditions (Prézelin and Matlick, 1983). The physical blending of surface phytoplankton communities with relatively high I_k values with deeper phytoplankton communities with lower I_k values will initially lead to a uniform value throughout the mixed layer. Should mixing continue, then phytoplankton would tend to photoadapt to the average irradiance of the mixed layer and the distinction between high and low light cells would disappear. However, any restratification of the water column would promote the redevelopment of high and low light adapted phytoplankton communities on time scales ranging from a few hours to a few days.

Reverse logic then argues that if water column I_ks were uniform, then complete water column mixing was or recently had been occurring.

Moving offshore along the 500 Line, MLDs shallowed from ca 80 m in waters below the Chl *a* patch to less than 60 m in waters near the edge of the continental shelf (Plate 3). Along the same transect, Chl *a* concentrations declined in surface waters and the turbid FWL was no longer evident. Therefore, the depth of the euphotic zone approached or exceeded that of the MLD on the outer shelf of the 500 Line (Plate 3). Elevated FUCO concentrations occurred, were just above the pycnocline and were associated with separate subsurface Chl *a* maxima on either side of the upwelling site at 500.140. All phytoplankton pigment concentrations were characteristically low in active upwelling sites where surface waters were transported to the surrounding area.

A fully illuminated upper mixed layer with recent inputs of inorganic nutrients is an optimal location for high rates of phytoplankton growth. Such growth appears to have occurred on the 500 Line in response to the wind-induced upwelling event, with diatom growth being favored over other groups of phytoplankton (Plate 2E). Greater diatom-specific growth in offshore waters would account for the drawdown of inorganic nutrients, especially silicate. Conversely, it would appear that the nearshore waters, although enriched for deep nutrients, would be less favorable growth environments for phytoplankton due to the shallow penetration of the light field into a deeper upper mixed layer. If so, it is tempting to suggest that a shift toward diatom-dominated communities would be possible nearshore but would take longer to achieve given the slow growth environment.

400, 300 and 200 Lines. Hydrographic data suggested that upwelling was occurring at two sites along or near the 400 Line. One upwelling site occurred near a topographical rise at the outer edge of the continental shelf (ca. 400.180) where the UCDW was forced onto the shelf by movement of the southern boundary of the ACC. Upwelling UCDW was also observed on the inner shelf of the 400 Line and was likely UCDW pushed onto the WAP continental shelf on the outer edge of the 300 Line which flowed, largely unrestricted, across a mid-shelf plateau until it encountered the sudden shallowing of the shelf around the island cluster at the inside edge of the 400 Line.

From a phytoplankton perspective, growth conditions should have improved as the MLDs shallowed near the upwelling sites on the 400 Line and the upper mixed layer was almost entirely within the euphotic zone (Plate 3). Two near-surface Chl *a* maxima were evident and were separated from each by an upwelling zone at 400.080 (Plate 1K). Both maxima were confined to waters above ca 40 m and characterized by $Si(OH)_4$:NO_3 ratios >2.25 (Plate 2G).

The Chl *a* max closest to shore (400.060) was located in shallow waters (<150 m; Fig. 5A) adjacent to a small archipelago of islands (Fig. 1). A FWL was again evident at stations closest to the islands (Plate 3, 400.040–400.080) and phytoflagellates, diatoms and chlorophytes contributed about equally to phytoplankton community composition. The second surface Chl *a* max was located mid-shelf between 400.120–140. It was coincident

with the only HEX + BUT max along the 400 Line. There were two subsurface FUCO maxima but they were not associated with Chl *a* or HEX + BUT maxima. The FUCO maxima were located at 400.060 and 400.180 and were positioned just above the MLDs and adjacent to the upwelling sites at 400.040 and 400.160, respectively. The $Si(OH)_4$:NO_3 ratios associated with the subsurface FUCO maxima were <2.25 (Plate 2G).

On the 300 Line the distribution of FUCO closely mimicked that of Chl *a*. The highest concentrations of both were located in a subsurface maximum 80–120 km offshore at locations on the shelf where MLDs were changing sharply. Given the partial bifurcation of the subsurface Chl *a* max at 100 km offshore, these may have represented two distinct subsurface communities of phytoplankton. The HEX + BUT concentrations were greatest in the subsurface waters less than 80 km from the shore line and were very low at all depths in the outer shelf. With one exception, no peridinin was detected along the 300 Line. Chl *b* was most abundant in subsurface waters within 80 km of the inner shelf and coincident with the area of highest HEX + BUT concentrations. Some Chl *b* was also detectable at or just below the MLD at the outer shelf stations.

Pigment concentrations along the 200 Line were determined at 40 km intervals rather than 20 km. Thus these data did not have sufficient spatial resolution for contouring pigment distribution along the 200 Line. However, analyses of individual vertical profiles suggest that Chl *a* concentrations were highest in subsurface waters within 120 km of the shore. HEX + BUT concentrations were highest inshore (>400 ng L^{-1}) and closely resembled the pattern of distribution of these pigments on the 300 Line. In contrast, highest accumulations of FUCO (>400 ng L^{-1}) occurred at the outermost stations at and beyond the continental shelf break (e.g. 600.120, 600.160, and 600.200). Chlorophytes, dinoflagellates, cryptophyres and prasinophytes were rare at any station location on the 200 Line.

f. Regional patterns in phytoplankton assemblages and their contribution to Chl a biomass

Diatom dominance, ranging from 60 to 90% of phytoplankton community biomass, occurred in regions characterized by bathymetric and recent wind-driven upwelling of UCDW. These diatom-dominated communities were associated with the lowest $Si(OH)_4$:NO_3 ratios (1.72 ± 0.32, $n = 115$); the lowest $Si(OH)_4$:PO_4 ratios (23.7 ± 4.0, $n = 113$); and highest NO_3:PO_4 ratios (13.9 ± 1.2, $n = 113$). For phytoflagellate-dominated communities the corresponding average $Si(OH)_4$:NO_3, $Si(OH)_4$:PO_4, and NO_3:PO_4 ratios were 2.45 ± 0.42 ($n = 84$), 30.4 ± 0.8 ($n = 84$) and 12.5 ± 1.3 ($n = 84$), respectively. The distinction between the nutrient availability of diatom-dominated and prymnesiophyte-dominated communities became even greater when samples with $>70\%$ of either phytoplankton grouping were considered separately.

Overall, diatoms accounted for more than two-thirds of the Chl *a* biomass within phytoplankton assemblages observed at the outer continental shelf stations of the 200, 300, and 400 Lines (Fig. 9A). However, increased dominance by diatoms did not translate into increased Chl *a* (Plate 1). The integrated Chl *a* biomass in the upper 100 m averaged

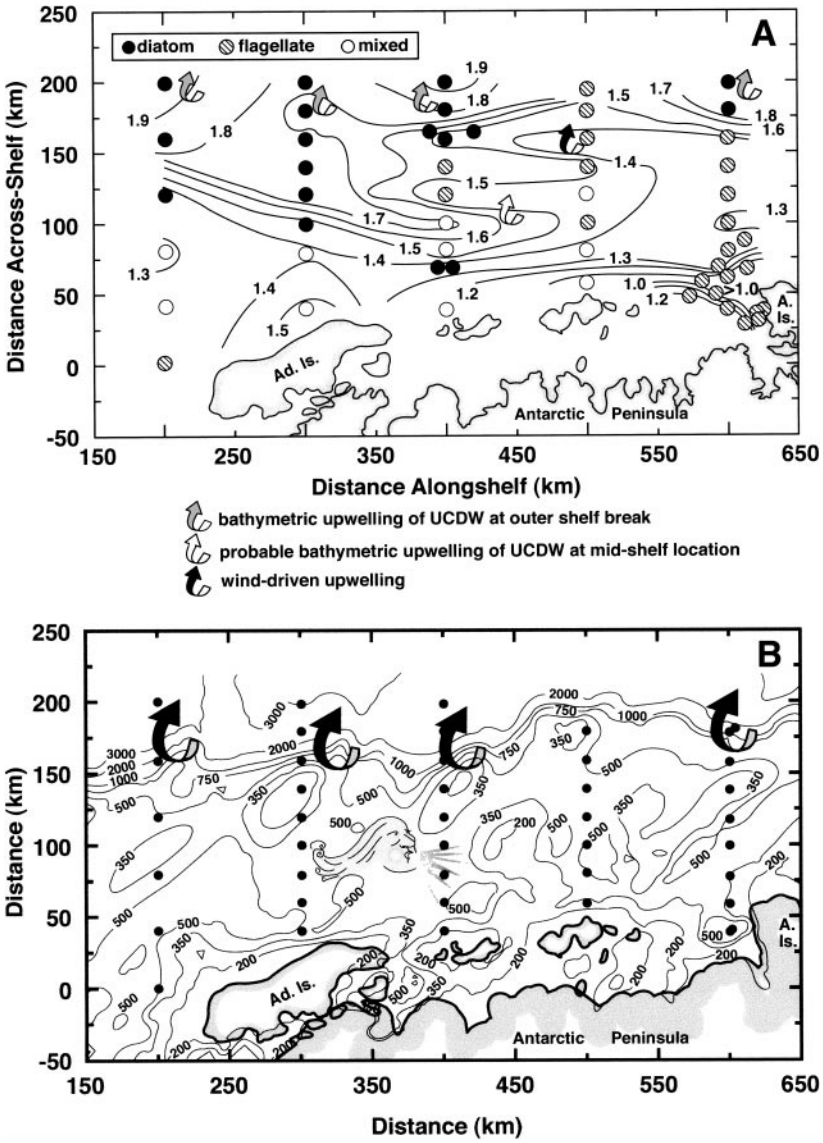

Figure 9. (A) Summary of dominant phytoplankton community composition overlaid on the temperature maxima distribution below 250 m. The diatom-dominated communities are comprised of >60% diatoms; flagellate dominated communities are comprised of >60% prymnesiophytes + pelagophytes; and mixed communities are those in which no algal group was >60%. The gray arrows indicate the sites where upwelling of UCDW was due to bathymetric effects. The site of recent wind-induced upwelling is indicated by the black arrow; the clear arrow indicates the site of potential wind-induced upwelling. (B) Summary schematic of the physical forcing that produces the phytoplankton community structure observed in January 1993. The black arrows indicate bathymetrically induced upwelling; the cartoon indicates the region that was potentially affected by wind-induced upwelling and the direction from which the upwelling favorable winds must come.

29.4 ± 6.8 mg m^{-2} or ca. half that of nearshore prymnesiophyte-dominated communities and about 20% that of spring blooms of diatoms occurring in nearby Palmer Basin (Moline and Prézelin, 1996) just a few weeks prior to our survey of the outer WAP continental shelf.

Phytoflagellates-dominated (70% to 90% of total phytoplankton biomass) communities occurred at nine stations along the 500 and 600 Lines (Fig. 9A), with dominance restricted to waters below the FWL. Six of the stations (600.120–140; 500.080–180) had a discernable deep MLD (ca 73 ± 12 m) and integrated water column Chl *a* biomass in the upper 100 m was 4.57 ± 1.74 mg Chl *a* m^{-2}. The remaining three stations had nearly identical Chl *a* biomass (e.g. 4.57 ± 1.49 mg m^{-2}) but no significant MLD within 200 m of the surface.

4. Discussion

a. General summary

i. Bathymetrically-induced upwelling. Intrusion of UCDW onto the WAP continental shelf in January to February 1993 provided a source of nutrient-rich water below 150 m. Upwelling of UCDW was observed at a minimum of four sites along the outer shelf, resulting in nutrients being introduced to the upper water column. The outer shelf sites at which upwelling was observed were areas of shallow bathymetry (less than 350 m) that were influenced by the southern boundary of the ACC. These locations also appeared to be a site for intrusion of UCDW onto the WAP continental shelf (Hofmann and Klinck, 1998a). Once on the outer shelf, the deeper water was driven upward by the shallowing topography, thereby introducing nutrients into the upper water column.

There appears to be correspondence between our findings and simultaneous observations reported by Kang and Lee (1995), who reported abrupt changes in phytoplankton taxonomic assemblages along two cross-shelf transects of the WAP continental shelf west of our study area. In their transects through the Bransfield Strait to the Drake Passage, diatom dominance of phytoplankton biomass increased abruptly on the outer shelf and shelf break seaward of the islands at the western end of the Bransfield Strait. At nearshore and mid-center locations, phytoflagellates dominated the phytoplankton assemblages. At both diatom-dominated locations described by Kang and Lee (1995), the density surfaces tilted upward above 100 m. These observations are consistent with our observations of diatom-dominated locations. However, without deeper profiles of the physical and chemical distributions, the presence of the UCDW along the transects occupied by Kang and Lee (1995) cannot be verified.

Preferential drawdown of $Si(OH)_4$ relative to NO_3 was indicated at each of the offshore upwelling sites, as evidenced by the reduction in the ambient ratio of these nutrients relative to the value it should have for unmodified UCDW (cf. Fig. 3B, Fig. 8). While the biomass accumulation was not always present at the upwelling sites, there was a shift to diatom-dominated communities at these locations and in nearby areas influenced by local circulation of near surface waters (Fig. 8). Upwelled water may have favored diatoms by providing supplemental silicate and/or iron.

We have shown that upwelling led to diatom dominance, but not necessarily abundance. We suggest significant diatom growth went undetected due to the influences of advection and/or grazing. Similar observations have been made by Brandini (1993) at Admiralty Bay, where iron enhancement did not lead to diatom blooms since microbial grazing kept algal biomass low. Likewise, Jennings *et al*. (1984) showed that the magnitude of nutrient depletion in the Weddell Sea indicated higher diatom primary production than did estimates based upon radiolabelled carbon uptake measurements. They concluded the underestimation was due to advection and/or grazing of algal biomass which would have otherwise accumulated on site.

ii. Wind driven upwelling. Waters characteristic of UCDW but not yet modified by biological activity or mixing were evident at 150 to 200 m along the inner portion of the 500 Line, as evidenced by their observed $Si(OH)_4$:NO_3 ratios between 2.75 and 3.0. Furthermore, these high $Si(OH)_4$:NO_3 ratios extended up to within 50 m of the surface in these areas, with this nutrient-rich water reaching the surface at two locations along the inner portion of the 500 Line. The high $Si(OH)_4$:NO_3 ratio and the vertical distribution of the nutrients strongly suggested that the area had experienced very recent upwelling. However, the inner 500 Line was far removed from the shelf break and the southern ACC boundary. Thus, upwelling in this region must be from physical forcing different from the bathymetric effects that occur at the outer shelf upwelling sites.

Since the winds overlying the WAP shelf are predominately from the north-northeast and therefore favorable to downwelling, the possibility of wind-induced upwelling would seem unlikely. However, during the time that the 500 Line was occupied in the 1993 austral summer, the wind direction had reversed and winds were from the south-southwest, which was upwelling favorable (cf. Fig. 2). The occurrence of the appropriate wind stress would rapidly upwell this water, resulting in injection of nutrients into the upper water column (Fig 9B). The bathymetry along the inner 500 Line (cf. Fig. 1) forms a semi-enclosed deep basin with bottom depths $\geq$500 m. The deep basin is continuous with the outer shelf, which allows UCDW to flood this area as it intrudes onto the shelf (Fig. 9A, B). Over time this water likely mixes slowly with the overlying AASW (Smith *et al.,* 1999).

The south-southeastward wind event, observed in January 1993, was the only upwelling-favorable wind event that occurred during the one-month interval of the regional sampling. These wind reversals are relatively unusual, occurring only 3 to 5 times with durations of 2 to 4 days during the austral summer (Smith, 1999). Thus, while episodic wind-induced upwelling does occur on the WAP continental shelf, it may not be a routine feature of the circulation of this shelf.

Inshore of wind-driven upwelling on the 500 Line, deep water nutrients rose to within 60–70 m of the surface (Fig. 6D, E, F). At these locations (Plate 5; 500.060–500.100) sampled prior to the wind event, diatoms were a very minor component of phytoplankton communities sampled down to 100 m. Phytoflagellates dominated these waters. Farther offshore in the area of wind-driven upwelling on the 500 Line, the proportionality of

diatoms increased significantly at depths below the 1% light field and the shallower MLD (Plate 2; 500.120 to 500.160).

Diatoms were found all along the 500 Line and, in fact, everywhere in the study area. They did not appear to become dominant until the physical conditions were such that nutrient inputs were of sufficient quantity and duration to allow for their preferential growth and a resulting shift in community composition. The high nutrient content of the inner shelf waters on the 500 Line represent very recent injections of large quantities of inorganic nutrients which had not yet been utilized to shift phytoflagellate-dominated communities toward diatom-dominated communities. Conversely, diatom-dominated communities (regardless of the biomass associated with them) likely reflect assemblages that reflect significant prior drawdown of inorganic nutrients at that location.

iii. Nonupwelling sites. At the nonupwelling sites, the phytoplankton communities were a mixture of prymnesiophytes and pelagophytes, with or without less abundant dinoflagellates or chlorophytes and the rarely occurring prasinophytes. These communities were found along the boundary between the modified UCDW and the inner shelf waters and along the boundary between modified UCDW and the shelf waters to the north toward Bransfield Strait (Fig. 9A). Phytoflagellates also dominated the phytoplankton community in the vicinity of Anvers Island, that is influenced by southerly flow onto the shelf from the Gerlache Strait and modified by glacial ice melt. The regions where phytoflagellate dominated tended to have shallow topography which restricted the flow of the modified UCDW water into these areas (cf. Fig. 1).

A *general conclusion* that emerges from the intercomparison of the hydrographic, nutrient, phytoplankton biomass, and pigment distributions is that diatom-enriched communities occur on the WAP only at locations where the physical forcing is allowing injection of UCDW into the upper water column (Fig 9). An additional general conclusion is that significant increases in diatom abundances and the development of diatom-dominated communities are probably site-specific on the west Antarctic shelf and episodic in nature. Site-specific enhancement of diatom growth (and hence dominance) may or may not lead to localized accumulations of diatom biomass, depending upon whether significant grazing pressure and/or surface advection are also evident. It is now clear that attempts to construct organic carbon or nutrient budgets for this region *must* include consideration of the small scale nature of the features that are responsible for creating or disrupting the conditions conductive to phytoplankton biomass accumulation and hence primary production.

b. Linkages to higher trophic levels

During January–February 1993, the distribution and size frequency of Antarctic krill, which was the dominant herbivore in this region, were measured simultaneously with the hydrographic and phytoplankton distributions (Lascara *et al.*, 1999). The distribution of the mode of the krill size frequency (Fig. 10) showed that the outer shelf locations were dominated by large (40–50 mm) and reproducing krill and that medium (25–35 mm) and

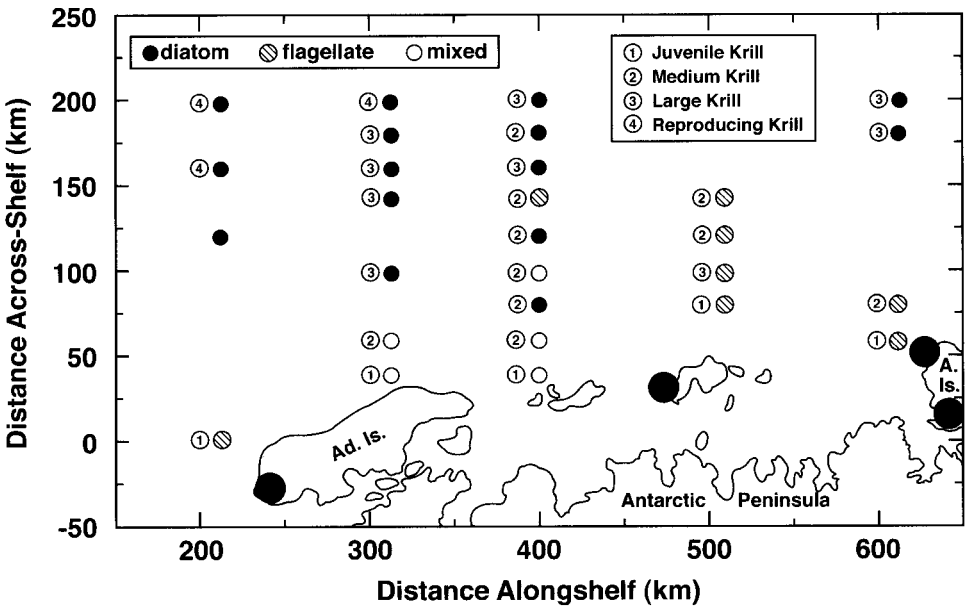

Figure 10. Distribution of phytoplankton community composition and corresponding krill distribution derived from the length frequency analyses presented in Lascara *et al.* (1999). Also shown are the locations of major Adélie penguin colonies (large circles) as given in Fraser and Trivelpiece (1996).

juvenile krill dominated the inner shelf locations. Thus, the larger krill were coincident with the upwelling areas where diatom-enriched phytoplankton communities were observed. The only exception was a site on the inner 500 Line; however, this site was the center of wind-induced upwelling at which a subsurface diatom bloom was developing. The smaller krill were associated with locations at which phytoflagellates dominated the phytoplankton assemblage.

The co-occurrence of large krill with diatom-enriched phytoplankton communities and smaller krill with phytoflagellate-dominated communities makes it tempting to conclude that the observed correspondences were a manifestation of selective feeding by the herbivore. Indeed the low phytoplankton biomass observed at the upwelling sites suggests that intense grazing pressure was occurring. Recent studies (Atkinson and Snÿder, 1997; Atkinson *et al.,* 1999) show Antarctic krill to be omnivores, so the processes underlying this observed predator-prey correspondence may be more complex than simple preference for particular food type.

An alternative possibility was that selective grazing was less important to krill distribution than the fact that the upwelling centers represent a persistent and dependable supply of food for organisms, such as Antarctic krill. The upwelling that occurred along the outer portions of the 200, 300, 400 and 600 Lines, was produced by the interaction of the ACC with shallowing topography at the shelf edge. Thus, as long as the ACC was near some

portion of the shelf region, upwelling, with its corresponding diatom-dominated phytoplankton community, will occur.

The larger Antarctic krill, which are capable swimmers, are known to migrate to the shelf edge within 50 m of the surface during the austral summer. Siegel (1988) suggested that this migration may be in response to reduced food on the inner shelf that cannot support the larger krill. It is possible that this migration was subject to selective pressure as the larger krill seek out a predictable and dependable food source that allowed them to maintain themselves in what was otherwise a food-poor environment. The occurrence of large krill at the wind-induced upwelling site on the inner 500 Line suggests that this is another site where krill may find a quasi-dependable food source in their offshore migration.

The occurrence of reproducing krill at the outer shelf was consistent with other observations that show that these animals spawn at the shelf edge to take advantage of the warmer UCDW for embryo development (Hofmann *et al.,* 1992). The current direction at the outer shelf was north-northeast and this forms the outer limb of the clockwise gyre that overlies the WAP shelf (Smith *et al.,* 1999). Superimposed on this gyre was a weaker diffusive circulation that was directed onshore at depth. This across-shelf circulation arises from the need to maintain the heat and salt balances on this shelf (Smith *et al.,* 1999). Thus, krill embryos which are released at the shelf edge and then sink to 200–300 m before hatching (Hofmann *et al.,* 1992), may be transported north-northeast and onshore, where they could become entrained in the clockwise gyre on the shelf. This provides an explanation, other than food selection, for the occurrence of the juvenile and medium krill at the nonupwelling sites along the inner shelf.

Adélie penguins are dependent on Antarctic krill as their food source. Therefore regions that provide dependable food for krill, will in turn provide a dependable food supply for the Adélie penguin. Adélie penguins have a foraging range of 100–150 km (Fraser and Trivelpiece, 1996). Their primary colonies along the WAP are in locations (Fig. 10) for which this foraging range will allow access to regions of dependable upwelling.

c. Relationship to larger scale Antarctic circulation

Upwelling along the outer portion of the WAP continental shelf is driven by the ACC, which was located at the outer shelf edge in this region of the Antarctic. Thus, other sites around the Antarctic where the southern portion of the ACC nears the shelf edge have the potential for similar upwelling. Orsi *et al.* (1995) provide the climatological distribution of the southern ACC front (SAACF) and southern ACC boundary (Bndy), as determined from historical hydrographic observations (Fig. 11). This distribution shows that the SACCF and Bndy near the Antarctic continent, and hence the shelf edge, between 40E and 80E, 120E and 180E, and 140W to 60W (Fig. 11).

Regions where the southern boundary of the ACC approaches the continental shelf edge are potential sites of shelf break upwelling and, hence, enhanced biological production. Indirect evidence in support of increased biological production is provided by the

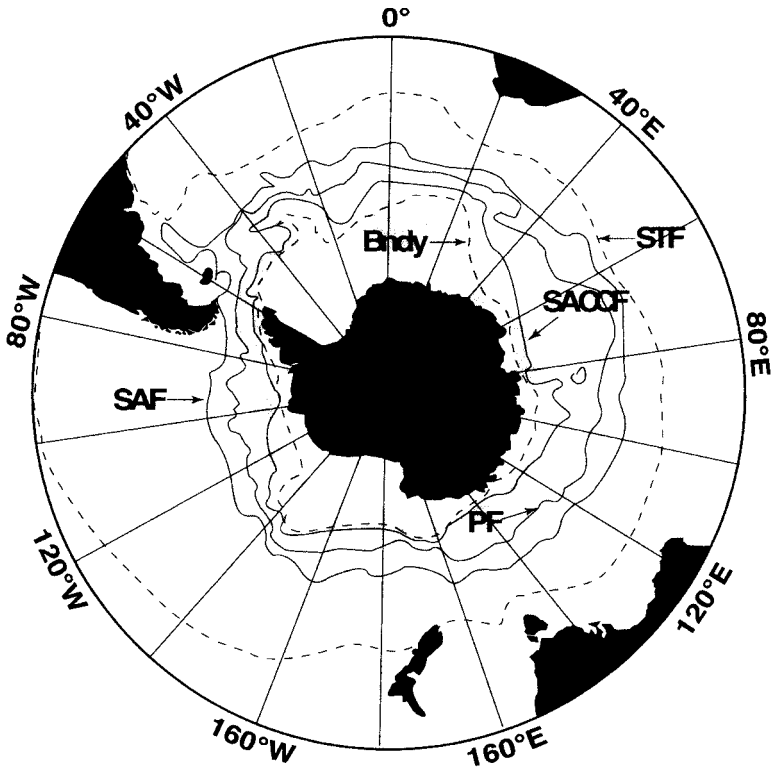

Figure 11. Distribution of the Subtropical Front (STF), Subantarctic Front (SAF), Polar Front (PF), southern Antarctic Circumpolar Current Front, (SACCF), and the southern Antarctic Circumpolar Current Boundary (Bndy) as given in Orsi *et al.* (1995). The shaded regions represent the distribution of regions with high concentrations of Antarctic krill as described in Everson and Miller (1994).

distribution of regions of high concentrations of Antarctic krill given in Everson and Miller (1994) (Fig. 11). The high krill regions coincide with the areas where the SACCF and Bndy are near the continent, and the krill regions are always found to the southern side of these fronts. This krill-ACC correspondence, while qualitative, is suggestive of possible mechanistic linkages that warrant further study. The exception to the shelf break upwelling-krill relationship was the correspondence of high krill concentrations with the SACCF and Bndy to the east of the Antarctic Peninsula and across the Scotia Sea (Fig. 11), which is believed to be the result of transport of krill from the Antarctic Peninsula by the SAACF (Murphy *et al.*, 1998; Hofmann *et al.*, 1998).

Variability in frequency, magnitude and duration of upwelling along the Antarctic continental shelf break is linked to variability in the location of the ACC. Hydrographic observations from the WAP region (Hofmann and Klinck, 1998a) show that the southern ACC boundary is at times located seaward of the shelf break. At these times, shelf break

upwelling would be expected to cease, as is observed for other continental shelf regions that are influenced by strong boundary currents (Atkinson, 1977). The core of the ACC is known to migrate north and south by as much as 100 km in three months (Hofmann and Whitworth, 1985), which could potentially interrupt or enhance shelf edge upwelling along portions of the Antarctic continental shelf as the SACCF and Bndy adjust location. Thus, monitoring the location of the SACCF in a specific region may provide an approach for estimating potential upwelling and related biological production. However, during periods of decreased ACC-related upwelling, episodic wind-induced upwelling may be the mechanism that sustains the marine food web of the continental shelf. The relative importance of wind-induced upwelling for Antarctic coastal regions remains to be quantified.

d. Implications for Antarctic continental shelf systems

Intrusions of UCDW onto the WAP continental shelf via shelf break forcing from the ACC, and the subsequent upwelling of this water by interaction with shallow bathymetry, sets up a physical and chemical structure that can potentially support localized increases in biological production. This is very different from MLD dynamics and we are not implying the MLD was the determinant of biological activity in this shelf region at this time of year; in fact quite the opposite. The number of potential sites, at which this type of upwelling could occur, suggests that the WAP continental shelf supports a significant production of phytoplankton biomass, but at time scales that are determined by the frequency of UCDW intrusions and space scales that are determined by bathymetric features. When extrapolated to other regions of the Antarctic where similar upwelling may exist, the picture of a productive continental shelf emerges. The addition of episodic wind-induced upwelling provides an additional mechanism to further enhance biological production of the Antarctic continental shelf. Thus, when viewed as a system of many localized, productive upwelling sites, the Antarctic shelf likely produces phytoplankton biomass that is in excess of what is needed to support the diverse food web of the higher trophic levels. Hence, the question to ask may be what is the fate of the excess organic carbon, rather than is there enough organic carbon.

At the upwelling sites on the WAP continental shelf, diatoms tend to dominate the phytoplankton community composition, but the duration of the January–February 1993 study was not sufficient to determine what underlies this dominance. The predominance of diatoms in other upwelling areas has been noted and it has been suggested to result from differential sinking of cells along upwelling plumes and/or rapid growth responses to upwelled nutrients (e.g. Smith *et al.*, 1987). The available data from the WAP suggest that diatom dominance at the upwelling centers may be related to silicate and/or a micronutrient, such as iron, that was upwelled with UCDW. If correct, there are implications for what is controlling diatom dominance of phytoplankton assemblages in other regions, such as the wind-driven upwelling centers of eastern boundary current regions, where deep oceanic water, that is presumably enriched in macro and micronutrients, is upwelled.

Perhaps the most intriguing aspect of the patterns and correlations derived from this analysis was the coupling of the structure of the physical environment through to the higher trophic levels. The mechanisms underlying this coupling remains to be determined, but it is clear that the ecology and biology of the components of the marine food web of the Antarctic continental shelf cannot be studied in isolation from one another. The real message from our analyses is that sampling of systems such as the Antarctic continental shelf needs to be done at space and time scales that are consistent with the physical and biological dynamics of the system.

Acknowledgments. This research was supported by the National Science Foundation, Office of Polar Programs grants OPP-9614938 (BBP) and OPP-9618383 (EEH). We thank the crew of the R/V *Polar Duke* and the scientists on the cruise for their helpful assistance. For hydrographic analyses, the computer resources and other facilities were provided by the Center for Coastal Physical Oceanography at Old Dominion University. We especially thank the SO16 primary productivity group (Nicholas Boucher, Tony Diem, Tanwas Hammond, Mark Moline and Sandi Roll) who prepared thousands of samples for biological and chemical analyses during the January 1993 cruise. Mark Moline worked endlessly to assure quality pigmentation analyses and quantification that were the starting point for the regression analyses and determination of phytoplankton community compositions presented herein. Analyses of nutrient samples were provided by the Marine Science Institute Analytical Laboratory at UCSB. Moe Gomez, John Kerfoot, Tim McGovern and Debbie Miller provided excellent technical assistance in data analyses and graphic preparations. The manuscript was improved thanks to valuable discussions with Mark Brzezinski and editorial comments by Julian Priddle and an anonymous reviewer.

REFERENCES

Atkinson, A. and R. Snÿder. 1997. Krill-copepod interactions at South Georgia, Antarctica, I. Omnivory by *Euphausia superba.* Mar. Ecol. Prog. Ser., *160,* 63–76.

Atkinson, A., P. Ward, A. Hill, A. S. Brierley and G. C. Cripps. 1999. Krill-copepod interactions at South Georgia, Antarctica, II. *Euphausia superba* as a major control on copepod abundance. Mar. Ecol. Prog. Ser., *176,* 63–79.

Atkinson, L. P. 1977. Modes of Gulf Stream intrusion into the South Atlantic Bight waters. Geophys. Res. Lett., *4,* 583–586.

Bidigare, R. R., J. L. Iriarte, S.-H. Kang, D. Karentz, M. E. Ondrusek and G. A. Fryxell. 1996. Phytoplankton: quantitative and qualitative assessment, *in* Foundations for Ecological Research West of the Antarctic Peninsula, R. Ross, E. Hofmann and L. Quetin, eds., Amer. Geophys. Union, Antarctic Research Series, *70,* 173–198.

Brandini, F. P. 1993. Phytoplankton biomass in an Antarctic coastal environment during stable water conditions-implications for the iron limitation theory. Mar. Ecol. Prog. Ser., *93,* 267–275.

Buma, A. G. J., P. Tréguer, G. W. Kraay and J. Morvan. 1990. Algal pigment patterns in different water masses of the Atlantic sector of the Southern Ocean during fall 1987. Polar Biol., *11,* 55–62.

Claustre, H., M. A. Moline and B. B. Prézelin. 1997. Sources of variability in the column photosynthetic cross section for Antarctic coastal waters. J. Geophys. Res., *102* (C11), 25047–25060.

Costa, D. P. and D. E. Crocker. 1996. Marine mammals in the Southern Ocean, *in* Foundations for Ecological Research West of the Antarctic Peninsula, R. Ross, E. Hofmann and L. Quetin, eds., Amer. Geophys. Union, Antarctic Research Series, *70,* 287–301.

de Baar, H. J. W., J. T. M. de Jong, D. C. E. Bakker, B. M. Löscher, C. Veth, U. Bathmann and V. Smetacek. 1995. Importance of iron for plankton blooms and carbon dioxide drawdown in the Southern Ocean. Nature, *373,* 412–415.

El-Sayed, S. Z. 1987. Biological productivity of Antarctic waters: present paradoxes and emerging paradigms. BIOMASS Sci. Ser., *71,* 1–22.

El-Sayed, S. Z. and G. A. Fryxell. 1993. Phytoplankton, *in* Antarctic Microbiology, Wiley-Liss, Inc., 65–122.

Everson, I. and D. G. M. Miller. 1994. Krill mesoscale distribution and abundance: results and implications of research during the BIOMASS Programme, *in* Southern Ocean Ecology: The BIOMASS Perspective, S. Z. El-Sayed, ed., Cambridge University Press, 129–143.

Fraser, W. R. and W. Z. Trivelpiece. 1996. Factors controlling the distribution of seabirds: winter-summer heterogeneity in the distribution of Adélie penguin populations, *in* Foundations for Ecological Research West of the Antarctic Peninsula, R. Ross, E. Hofmann and L. Quetin, eds., Amer. Geophys. Union, Antarctic Research Series, *70,* 257–272.

Haberman, K. L., R. M. Ross and L. B. Quetin. 1993. Palmer LTER: Grazing by the Antarctic krill *Euphausia superba* on *Nitzschia* sp. and *Phaeocystwas* sp. monocultures. Antarctic J. U. S., *27,* 217–219.

Hofmann, E. E., J. E. Capella, R. M. Ross and L. B. Quetin. 1992. Models of the early life history of *Euphausia superba*-Part I. Temperature dependence during the descent-ascent cycle. Deep-Sea Res., *39,* 911–941.

Hofmann, E. E. and J. M. Klinck. 1998a. Thermohaline variability of the waters overlying the West Antarctic Peninsula continental shelf, ocean, ice and atmosphere, *in* Interactions at the Antarctic Continental Margin, S. Jacobs and R. Weiss, eds., Amer. Geophys. Union, Antarctic Research Series, *75,* 67–81.

—— 1998b. Hydrography and circulation of the Antarctic continental shelf: 150E eastward to the Greenwich Meridian, *in* The Sea, The Global Coastal Ocean, Regional Studies and Synthesis, A. R. Robinson and K. H. Brink, eds., *11,* 997–1042.

Hofmann, E. E., J. M. Klinck, C. M. Lascara and D. A. Smith. 1996. Hydrography and circulation west of the Antarctic Peninsula and including Bransfield Strait, *in* Foundations for Ecological Research West of the Antarctic Peninsula, R. Ross, E. Hofmann and L. Quetin, eds., Amer. Geophys. Union, Antarctic Research Series, *70,* 61–80.

Hofmann, E. E., J. M. Klinck, R. A. Locarnini, B. Fach and E. Murphy. 1998. Krill transport in the Scotia Sea and environs. Antarctic Sci., *10,* 406–415.

Hofmann, E.E. and T. Whitworth III. 1985. A synoptic description of the flow through Drake Passage from year-long measurements. J. Geophys. Res., *90,* 7177–7187.

Holm-Hansen, O. and B. G. Mitchell. 1991. Spatial and temporal distribution of phytoplankton and primary production in the western Bransfield Strait region. Deep-Sea Res., *38,* 961–980.

Holm-Hansen and M. Vernet. 1992. RACER: Distribution, abundance, and productivity of phytoplankton in Gerlache Strait during austral summer. Antarctic J. U. S., *27,* 154–156.

Hutchins, D. A. and K. W. Bruland. 1998. Iron-limited diatom growth and silicate:nitrogen uptake ratios in a coastal upwelling regime. Nature, *393,* 561–564.

Jeffrey, S. W., R. F. C. Mantoura and S. W. Wright (eds.). 1997. Phytoplankton Pigments in Oceanography, UNESCO, Paris, France, 661 pp.

Jennings, J. C. Jr., L. I. Gordon and D. M. Nelson. 1984. Nutrient depletion indicates high primary productivity in the Weddell Sea. Nature, *308,* 51–54.

Johnson, K. S., R. L. Petty and J. Thomsen. 1985. Flow injection analysis for seawater macronutrients, *in* Mapping Strategies in Chemical Oceanography, A. Zirino, ed., Advances in Chemistry Series, *209,* 7–30.

Kang, S.-H. and S. H. Lee. 1995. Antarctic phytoplankton assemblage in the western Bransfield Strait region, February 1993: composition, biomass and mesoscale distributions. Mar. Ecol. Prog. Ser., *129,* 253–267.

Kellerman, A. K. 1996. Midwater fish ecology, *in* Foundations for Ecological Research West of the Antarctic Peninsula, R. Ross, E. Hofmann and L. Quetin, eds., Amer. Geophys. Union, Antarctic Research Series, *70,* 231–256.

Lascara, C. M., E. E. Hofmann, R. R. Ross and L. B. Quetin. 1999. Seasonal variability in the distribution of Antarctic krill, *Euphausia superba,* west of the Antarctic Peninsula. Deep-Sea Res., *46,* 925–949.

Lascara, C. M., R. C. Smith and D. Menzies. 1993a. XBT data collected aboard the R/V *Polar Duke* January–February 1993, CCPO Technical Report No. 93-03, Center for Coastal Physical Oceanography, Old Dominion University, 101 pp.

Lascara, C. M., R. C. Smith, D. Menzies, and K. S. Baker. 1993b. Oceanographic data collected aboard the R/V *Polar Duke* January–February 1993, CCPO Technical Report No. 93-02, Center for Coastal Physical Oceanography, Old Dominion University, 307 pp.

Lubimova, T. G., R. R. Makarov, V. V. Maslenikov, V. V. Shevtsow and K. V. Shust. 1982. The ecological peculiarities, stocks and role of *Euphausia superba* in the trophic structure of the Antarctic ecosystem, *in* Selected Papers Presented to the Scientific Committee of CCAMLR, 1982–1984, CCAMLR, Hobart, 391–505.

Mitchell, B. G. and O. Holm-Hansen. 1991. Observations and modeling of the Antarctic phytoplankton crop in relation to mixing depth. Deep-Sea Res., *38,* 981–1007.

Moline, M. A. and B. B. Prézelin. 1994. Palmer LTER: Impact of a large diatom bloom on macronutrient distribution in Arthur Harbor during austral summer 1991–1992. Antarctic J. US, *29,* 217–219.

—— 1996. Long-term monitoring and analyses of physical factors regulating variability in coastal Antarctic phytoplankton biomass, *in situ* productivity and taxonomic composition over subseasonal, seasonal and inter-annual time scales, Mar. Ecol. Prog. Ser., *145,* 143–160.

—— 1997. High-resolution time-series data for primary production and related parameters at a Palmer LTER coastal site: Implications for modeling carbon fixation in the Southern Ocean. Polar Biol., *17,* 39–53.

—— 2000. Optical fractionation of chlorophyll and primary production for coastal waters of the Southern Ocean. Polar Biol., *23,* 129–136.

Moline, M. A., B. B. Prézelin, O. Schofield and R. C. Smith. 1997. Temporal dynamics of coastal Antarctic phytoplankton: Environmental driving forces through a 1991–1992 summer diatom bloom on the nutrient and light regime, *in* Antarctic Communities, B. Battaglia, J. Valencia and D. W. H. Walton, eds., Cambridge Press, London, 67–72.

Moline, M. A., O. Schofield and N. P. Boucher. 1998. Photosynthetic parameters and empirical modeling of primary production: a case study on the Antarctic Peninsula shelf. Antarctic Sci., *10,* 45–51.

Morris, D. J. and J. Priddle. 1984. Observations on the feeding and molting of the Antarctic krill, *Euphausid superba* Dana, in winter. British Antarctic Survey Bull., *65,* 57–63.

Mura, M. P., M. P. Satta and S. Agusti. 1995. Water-mass influences on summer Antarctic phytoplankton biomass and community structure. Polar Biol., *15,* 15–20.

Murphy, E. J., J. L. Watkins, K. Reid, P. N. Trathan, I. Everson, J. P. Croxall, J. Priddle, M. A. Brandon, A. Brierley and E. Hofmann. 1998. Interannual variability of the South Georgia marine ecosystem: biological and physical sources of variation in the abundance of krill. Fisheries Oceanogr., *7,* 381–390.

Nelson, D. M. and W. O. Smith, Jr. 1986. Phytoplankton bloom dynamics of the western Ross Sea ice-edge. Deep Sea Res., *33,* 1389–1412.

Nichols, P. D., J. H. Skerratt, A. Davidson, H. Burton and T. A. McMeekin. 1991. Lipids of cultured *Phaeocystwas pouchetii:* signatures for food-web, biogeochemical and environmental studies in Antarctica and the Southern Ocean. Phytochemistry, *30,* 3209–3214.

Nolting, R. F., H. J. W. de Baar, A. J. Van Bennekom and A. Masson. 1991. Cadmium, copper and iron in the Scotia Sea, Weddell Sea and Weddell/Scotia Confluence (Antarctica). Mar. Chem., *35,* 219–243.

Orsi, A. H., T. Whitworth III and W. D. Nowlin, Jr. 1995. On the meridional extent and fronts of the Antarctic Circumpolar Current, Deep-Sea Res., *42,* 641–673.

Perrin, R. A., P. Lu and H. J. Marchant. 1987. Seasonal variation in marine phytoplankton and ice algae at a shallow Antarctic coastal site. Hydrobiologia, *146,* 33–46.

Prézelin, B. B., N. P. Boucher and R. C. Smith. 1994. *Icecolors '90:* Marine primary production under the Antarctic ozone hole, *in* Ultraviolet Radiation and Biological Research in Antarctica, S. Weiler and P. Penhale, eds, Antarctic Res. Ser., *62,* 159–186.

Prézelin, B. B. and H. A. Matlick. 1983. Nutrient-dependent low light adaptation in the dinoflagellate, *Gonyaulax polyedra.* Mar. Biol., *74,* 141–150.

Prézelin, B. B., M. M. Tilzer, O. Schofield and C. Haese. 1991. The control of the production process of phytoplankton by the physical structure of the aquatic environment with special reference to its optical properties. Aquatic Sci., *53,* 1015–1621.

Priddle, J., F. Brandini, M. Lipski and M. R. Thorley. 1994. Pattern and variability of phytoplankton biomass in the Antarctic Peninsula region: an assessment of the BIOMASS cruises, *in* Southern Ocean Ecology: the BIOMASS Perspective, S. Z. El-Sayed, ed., Cambridge University Press, 49–61.

Ross, R. M., E. E. Hofmann and L. B. Quetin, eds. 1996. Foundations for Ecological Research West of the Antarctic Peninsula. American Geophysical Union, Antarctic Research Series, *70,* 448 pp.

Sakshaug, E., D. Slagstad, O. Holm-Hansen. 1991. Factors controlling the development of phytoplankton blooms in the Antarctic Ocean—A mathematical model. Mar. Chem., *35,* 259–271.

Siegel, V. 1988. A concept of seasonal variation of krill (*Euphasia superba*) distribution and abundances west of the Antarctic Peninsula, *in* Antarctic Ocean and Resource Variability, D. Sahrhage, ed. Springer-Verlag, 219–230.

Smith, D. A. 1999. Modeling and observations studies of sea ice-mixed layer interactions on the West Antarctic Peninsula Continental Shelf, Ph.D. dissertation, Old Dominion University.

Smith, D. A., E. E. Hofmann, J. K. Klinck and C. M. Lascara. 1999. Hydrography and circulation in the west Antarctic Peninsula continental shelf. Deep-Sea Res., *46,* 951–984.

Smith, R. C., K. S. Baker, W. R. Fraser, E. E. Hofmann, D. M. Karl, J. M. Klinck, L. B. Quetin, B. B. Prézelin, R. M. Ross, W. Z. Trivelpiece and M. Vernet. 1995. The Palmer LTER: A long-term ecological research program at Palmer Station, Antarctica. Oceanograph., *8,* 77–86.

Smith, R. C., R. R. Bidigare, B. B. Prézelin, K. S. Baker and J. M. Brooks. 1987. Optical characterization of primary productivity across a coastal front. Mar. Biol., *96,* 575–591.

Smith, R. C., C. R. Booth, and J. Starr. 1984. Oceanographic bio-optical profiling system. Applied Optics, *23,* 2791–2797.

Smith, R. C., H. M. Dierssen and M. Vernet. 1996. Phytoplankton biomass and productivity in the western Antarctic peninsula region, *in* Foundations for Ecological Research West of the Antarctic Peninsula, R. M. Ross, E. E. Hofmann and L. B. Quetin, eds., Amer. Geophys. Union, Antarctic Research Series, *70,* 333–356.

Smith, W. O. Jr., ed. 1990a. Polar Oceanography, Part A: Physical Science, Academic Press, Inc., San Diego, 406 pp.

—— 1990b. Polar Oceanography, Part B: Chemistry, Biology and Geology, Academic Press, Inc., San Diego, 760 pp.

Smith, W. O. Jr. and L. J. Gordon. 1977. Hyperproductivity of the Ross Sea (Antarctica) polyna during austral spring. Geophys. Res. Lett., *24,* 233–236.

Smith, W. O. Jr. and E. Sakshaug. 1990. Polar phytoplankton, *in* Polar Oceanography, Part B: Chemistry, Biology and Geology, W. O. Smith, Jr., ed., Academic Press, Inc., San Diego, 477–526.

Sommer, U. 1988. The species composition of Antarctic phytoplankton interpreted in terms of Tilman's competition theory. Oecologia, *77,* 464–467.

Sullivan, B., H. A. Matlick and B. B. Prézelin. 1994. Palmer LTER: Austral Winter 1993: Patterns of distribution of inorganic macronutrients, phytoplankton pigmentation, and photosynthetic activity in an ice-dominated ecosystem. Antarctic J. U. S., *29,* 207–209.

Tréguer, P. and G. Jacques. 1992. Dynamics of nutrients and phytoplankton, and fluxes of carbon, nitrogen and silicon in the Antarctic Ocean. Polar Biol., *12,* 149–162.

UNESCO. 1983. Algorithms for computation of fundamental properties of seawater, N. P. Fofonoff and R. C. Millard, Jr. eds., Tech. Pap. Mar. Sci., *44,* 53 pp.

Valiela, I. 1995. Marine Ecological Processes, 2nd ed., Springer-Verlag, NY, 640 pp.

Vaulot, D., J. L. Birrien, D. Marie, R. Casotti, M. J. W. Veldhuis, G. W. Kraay and M.-J. Chrétiennot-Dinet. 1994. Morphology, ploidy, pigment composition, and genome size of cultured strains of *Phaeocystwas* (Prymnesiophyceae). J. Phycol., *30,* 1022–1035.

Von Brökel, K. 1981. The importance of nanoplankton within the pelagic Antarctic ecosystem. Kiel Meeresforsch, *5,* 61–67.

Wilson, D. L., W. O. Smith, Jr. and D. M. Nelson. 1986. Phytoplankton bloom dynamics of the western Ross Sea ice edge-I. Primary production and species-specific production. Deep-Sea Res., *33,* 1375–1387.

Wright, S. W. and S. W. Jeffrey. 1987. Fucoxanthin pigment markers of marine phytoplankton analyzed by HPLC and HPTLC. Mar. Ecol. Prog. Ser., *38,* 259–266.

Wright, S. W., S. W. Jeffrey, R. F. C. Mantoura, C. A. Llewellyn, T. Bjornland, D. Repeta and N. Welschmeyer. 1991. Improved HPLC method for the analysis of chlorophylls and carotenoids from marine phytoplankton. Mar. Ecol. Prog. Ser., *77,* 183–196.

Received: *17 August, 1999;* revised: *25 February, 2000.*

Figures 4 through 7 and Plates 1 and 2 follow

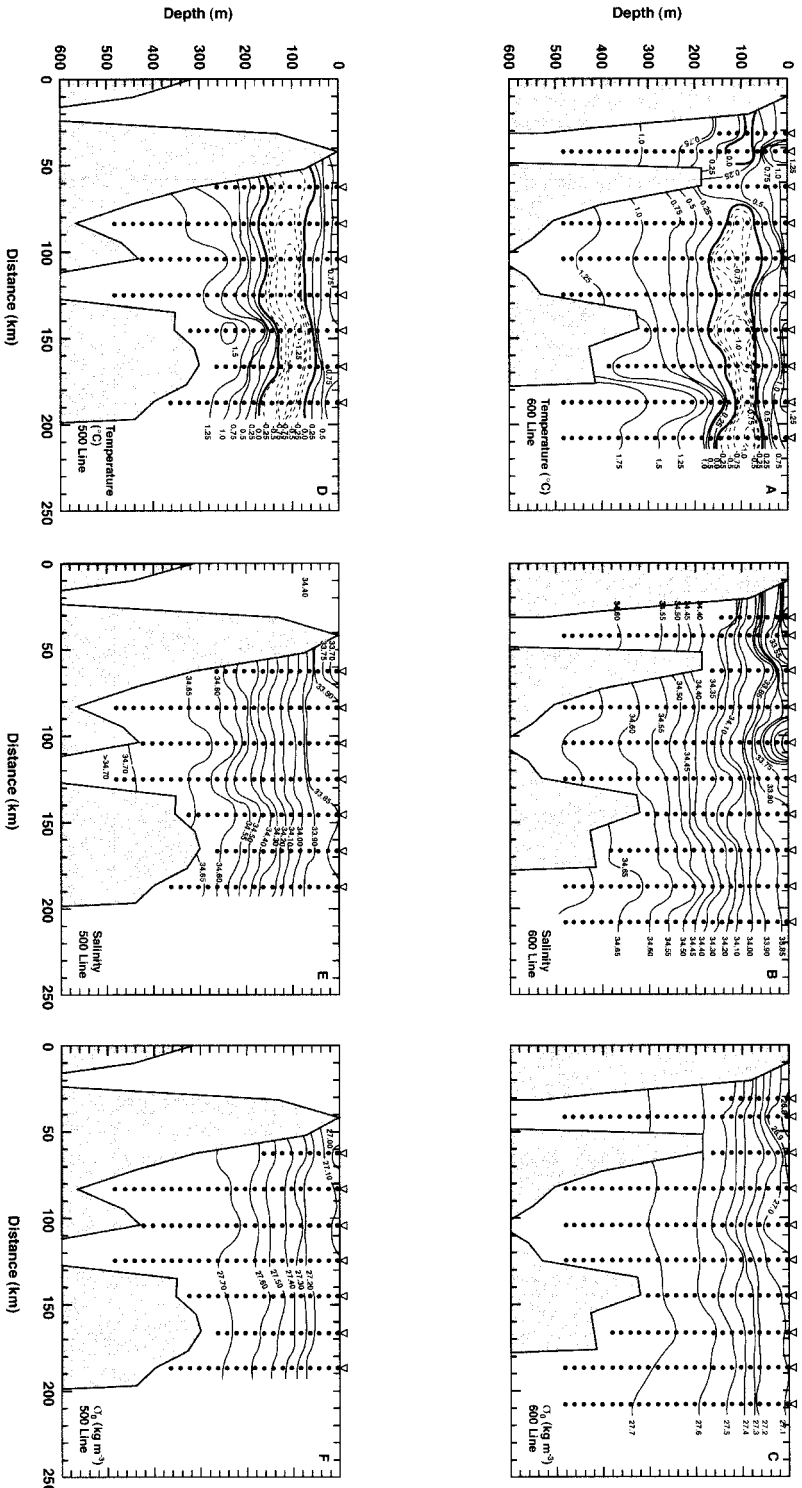

Figure 4. Vertical sections of temperature, salinity and potential density (σ_0) from the 600 (A, B, C) and 500 (D, E, F) transect lines. Contour intervals are 0.25°C, 0.1 ppt and 0.1 kg m^{-3}, respectively. Dashed contours indicate negative temperatures and the 0°C contour is denoted as a heavy line. Shading indicates bottom bathymetry. The station locations are indicated by the open triangles and the data distribution at each station used to construct the vertical section is shown by the filled circles.

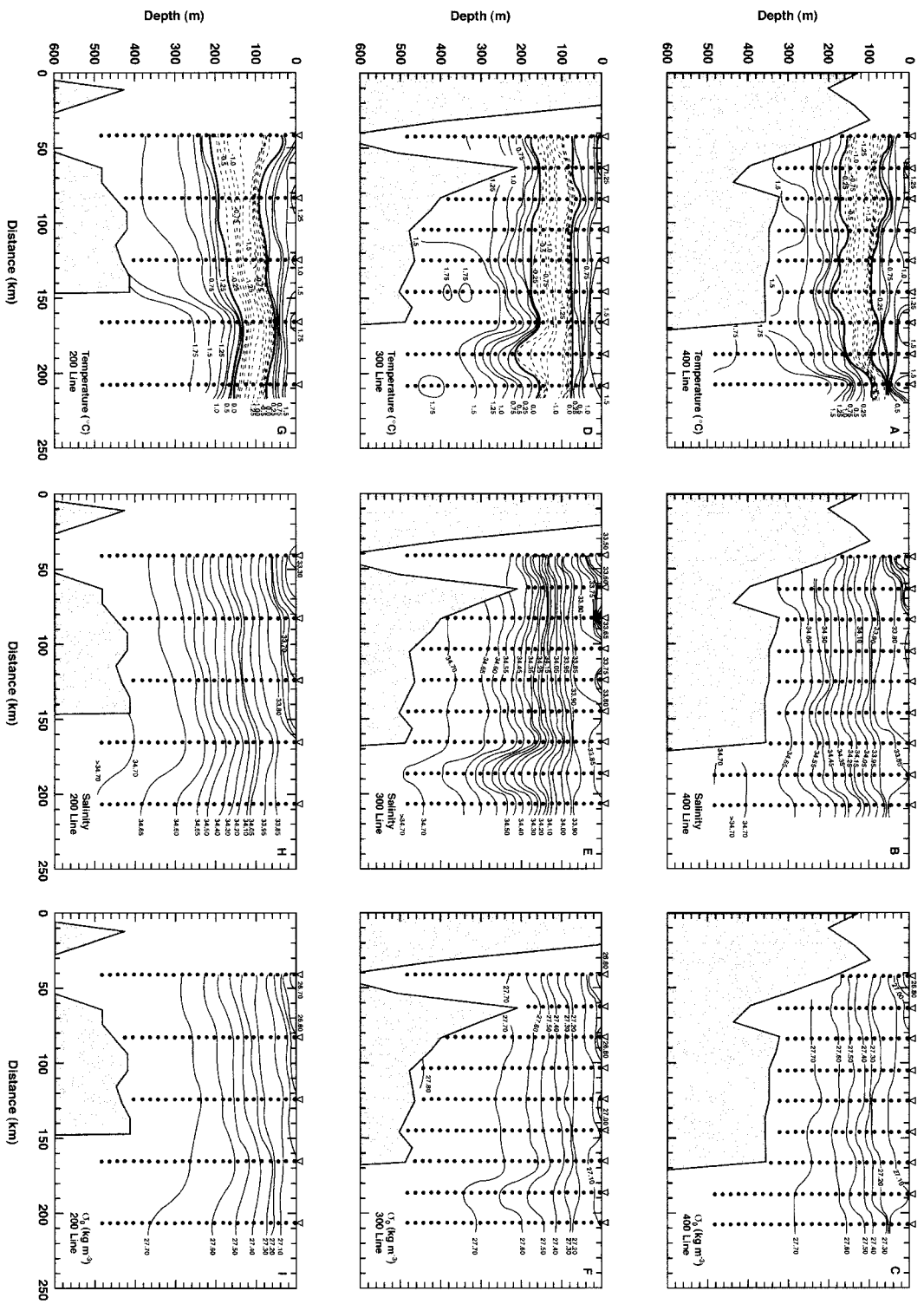

Figure 5. Vertical sections of temperature, salinity and potential density (σ_0) from the 400 (A, B, C), 300 (D, E, F) and 200 (G, H, I) transect lines. Contour intervals are 0.25°C, 0.1 ppt and 0.1 kg m^{-3}, respectively. Dashed contours indicate negative temperatures and the 0°C contour is denoted as a heavy line. Shading indicates bottom bathymetry. The station locations are indicated by the open triangles and the data distribution at each station used to construct the vertical section is shown by the filled circles.

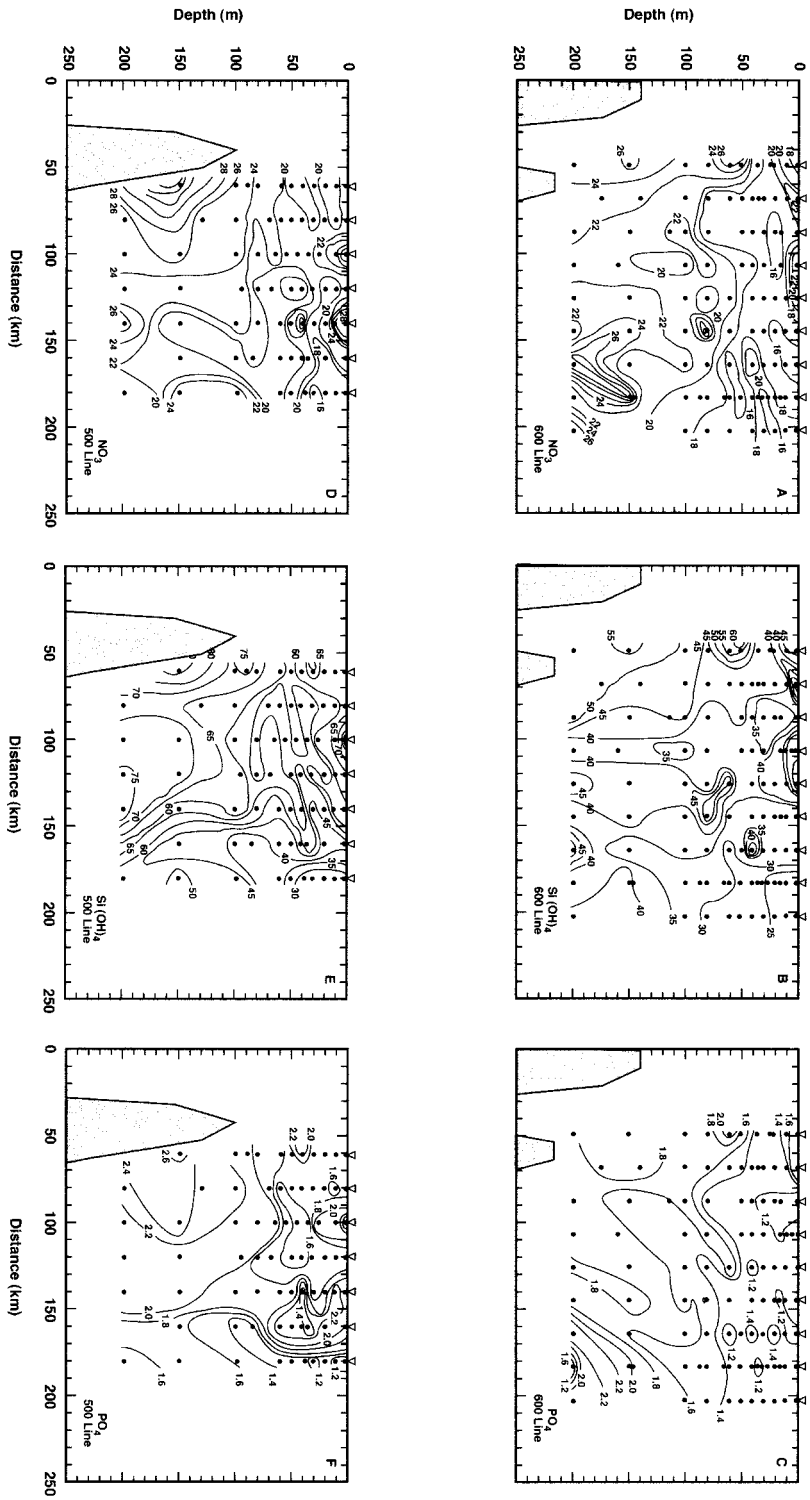

Figure 6. Vertical sections of ambient nitrate, silicate, and phosphate distribution on the 600 (A, B, C) and 500 (D, E, F) transect lines. Contour intervals are 2 mmol m^{-3}, 5 mmol L^{-1}, and 0.2 mmol L^{-1}, respectively. Shading indicates bottom bathymetry. The station locations are indicated by the open triangles and the data distribution at each station used to construct the vertical section is shown by the filled circles.

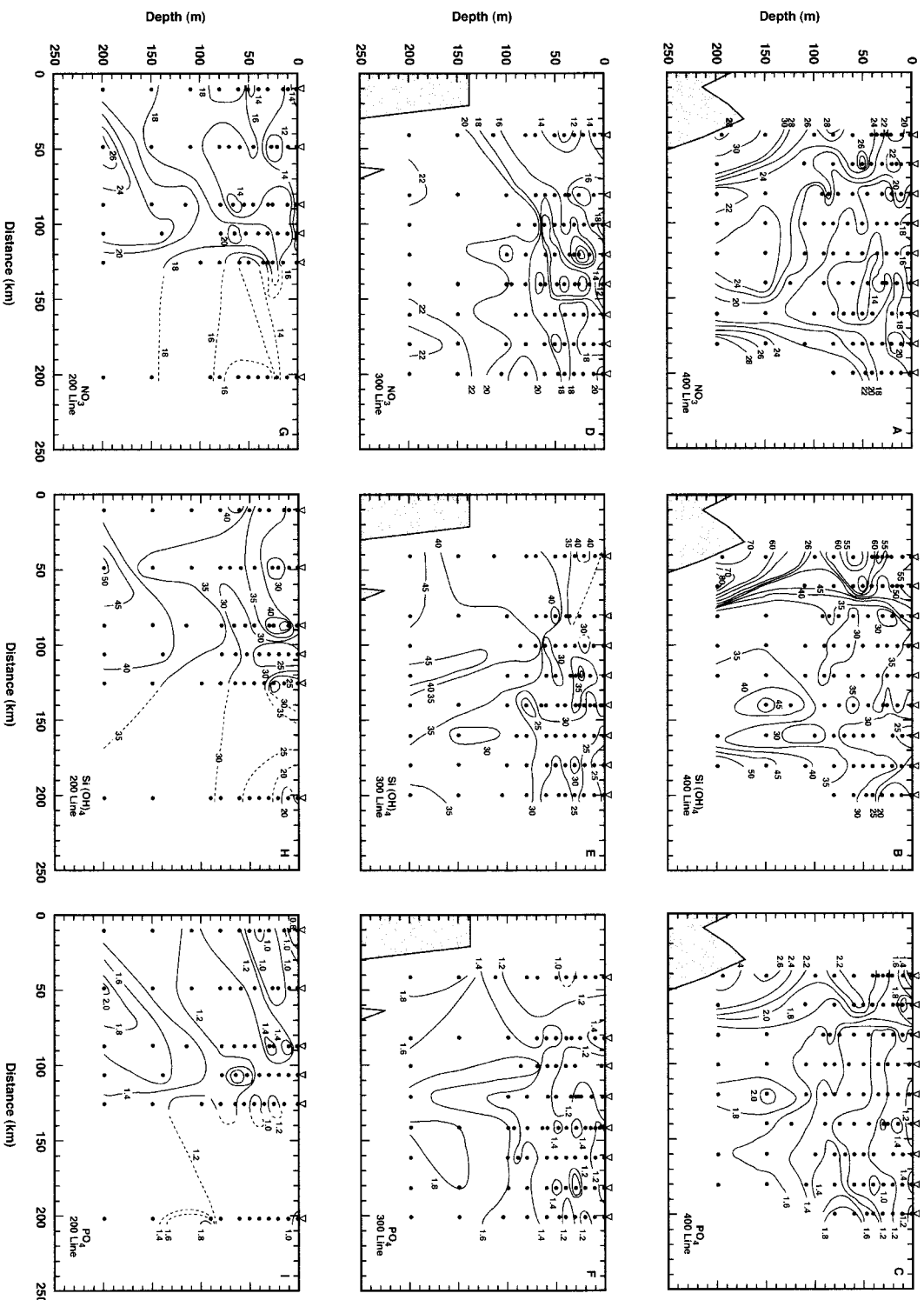

Figure 7. Vertical sections of nitrate, silicate, and phosphate distribution on the 400 (A, B, C), 300 (D, E, F) and 200 (G, H, I) lines. Contour intervals are 2 mmol m^{-3}, 5 mmol m^{-3}, and 0.2 mmol m^{-3}, respectively. Shading indicates bottom bathymetry. The station locations are indicated by the open triangles and the data distribution at each station used to construct the vertical section is shown by the filled circles.

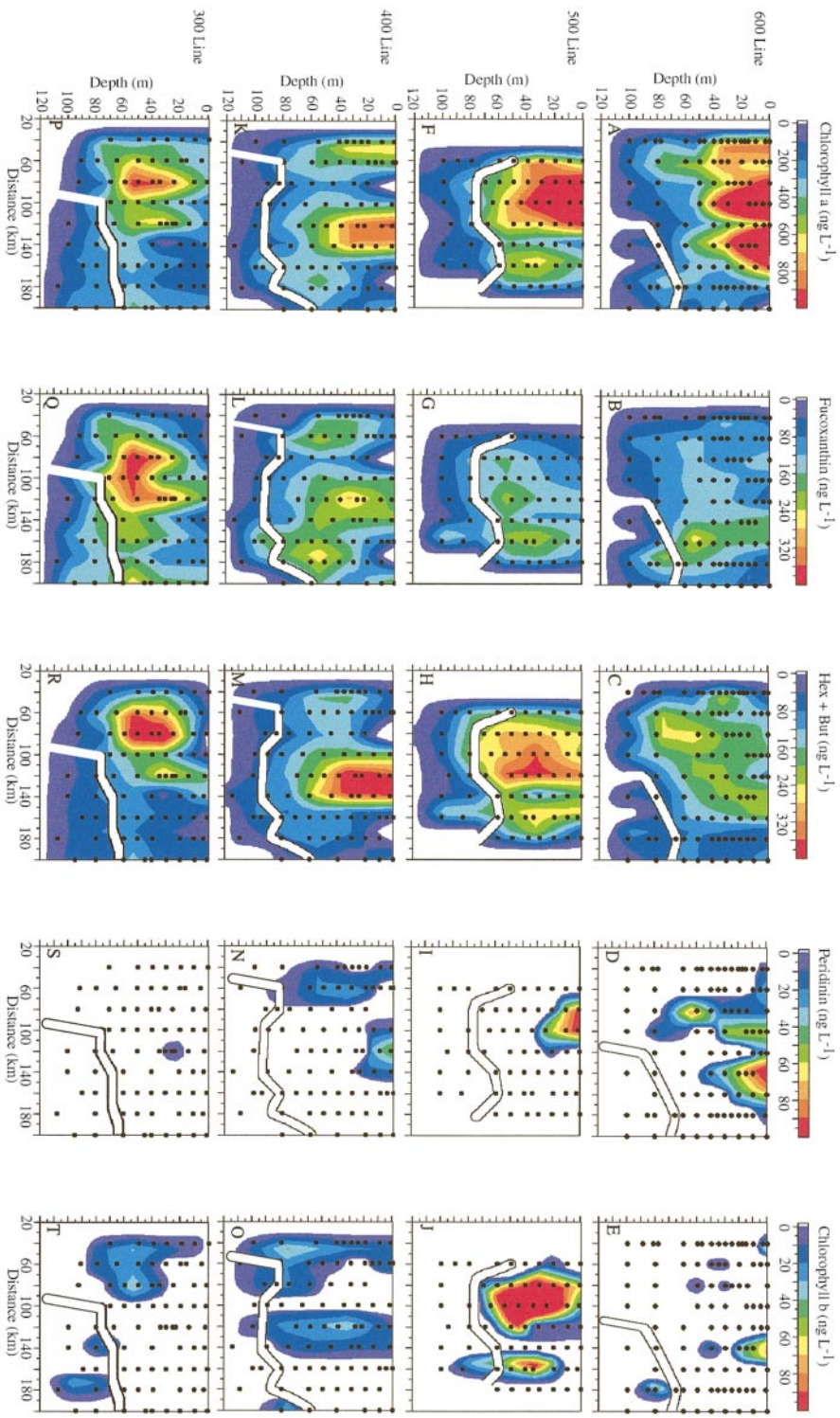

Plate 1. Vertical sections of the distribution of the most abundant phytoplankton pigment biomarkers constructed from measurements made at stations along the 600 (top) to 300 (bottom) transect lines. The sampling grid is shown for each transect. Concentration ranges for the pigment contours are given along the top axis. Note differences in the scales used for the different pigments. The HEX + BUT designation indicates the combined concentrations of 19′-hexanoyloxyfucoxanthin and 19′-butanoyloxyfucoxanthin. The white band represents the depths of the mixed layer.

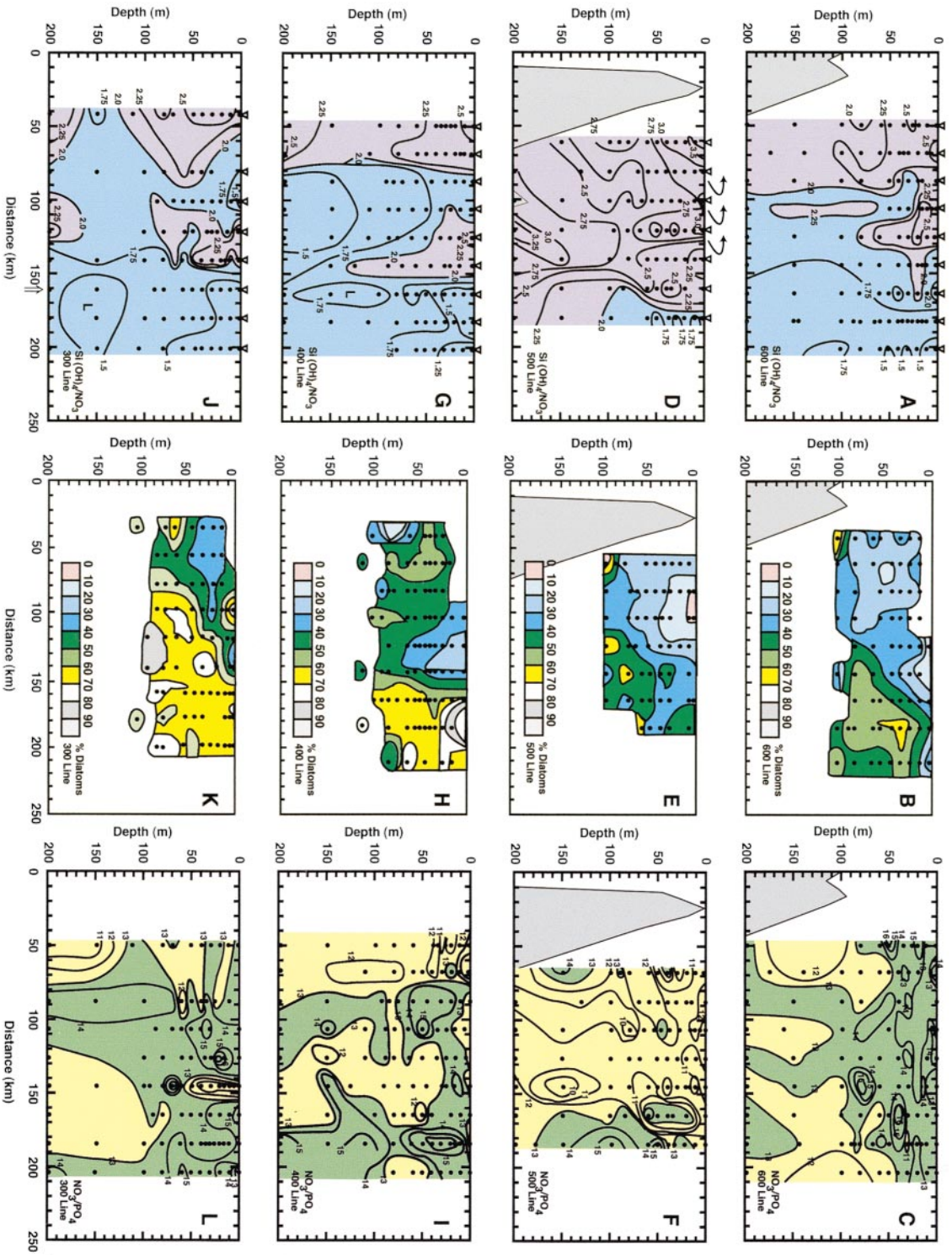

Plate 2. Vertical distributions of the ambient $Si(OH)_4$:NO_3 ratio (left), the % contribution made by diatoms to the overall phytoplankton community (middle), and the ambient NO_3:PO_4 ratio (right) along the 600 Line (A, B, C), 500 Line (D, E, F), 400 Line (G, H, I), and 300 Line (J, K, L) transects. Contour intervals for the $Si(OH)_4$):NO_3 ratio and NO_3:PO_4 ratio are 0.25 and 1.0, respectively. The data distribution at each station used to construct the vertical section is shown by the filled circles. Grey shading indicates bottom bathymetry. Shading for the $Si(OH_4)$:NO_3 ratio indicates regions greater than (purple) and less than (blue) 2.0. Shading for the NO_3:PO_4 ratio indicates regions greater than (green) and less than (yellow) 13.0.